FUSE

Fungal Systematics and Evolution

VOLUME 10
DECEMBER 2022
PAGES 177–215

doi.org/10.3114/fuse.2022.10.08

Fusarium diversity associated with the *Sorghum-Striga* interaction in Ethiopia

L. Lombard[1,2*], R. van Doorn[1], J.Z. Groenewald[1], T. Tessema[3], E.E. Kuramae[4,5], D.W. Etolo[4,6], J.M. Raaijmakers[4,7], P.W. Crous[1,6,8*]

[1]Westerdijk Fungal Biodiversity Institute, Uppsalalaan 8, 3584CT Utrecht, The Netherlands
[2]Dutch General Inspection Service for agricultural seeds and seed potatoes (NAK), Randweg 14, 8304 AS, Emmeloord, The Netherlands
[3]Ethiopian Institute of Agricultural Research, Addis Ababa, Ethiopia
[4]Netherlands Institute of Ecology (NIOO-KNAW), Department of Microbial Ecology, Wageningen, 6708 PB, The Netherlands
[5]Institute of Environmental Biology, Ecology and Biodiversity, Utrecht University, 3584 CH, Utrecht, The Netherlands
[6]Wageningen University and Research Centre (WUR), Laboratory of Phytopathology, Droevendaalsesteeg 1, 6708 PB Wageningen, The Netherlands
[7]Institute of Biology, Leiden University, Leiden 2333 BE, The Netherlands
[8]Microbiology, Department of Biology, Utrecht University, Padualaan 8, Utrecht, 3584 CH, The Netherlands

*Corresponding author: l.lombard@nak.nl, p.crous@wi.knaw.nl

Key words:
biological control agent
molecular phylogeny
systematics
three novel taxa

Abstract: *Sorghum* production is seriously threatened by the root parasitic weeds (RPWs) *Striga hermonthica* and *Striga asiatica* in sub-Saharan Africa. Research has shown that *Striga* control depends on eliminating its seed reserves in soil. Several species of the genus *Fusarium* (*Nectriaceae, Hypocreales*), which have been isolated from diseased *Striga* plants have proven to be highly pathogenic to all developmental stages of these RPWs. In the present study 439 isolates of *Fusarium* spp. were found associated with soils from *Sorghum* growing fields, *Sorghum* rhizosphere, or as endophytes with *Sorghum* roots and seeds, or as endophytes of *Striga* stems and seeds. Based on multi-locus phylogenies of combinations of *CaM*, *tef1*, *rpb1* and *rpb2* alignments, and morphological characteristics, 42 species were identified, including three species that are newly described, namely *F. extenuatum* and *F. tangerinum* from *Sorghum* soils, and *F. pentaseptatum* from seed of *Striga hermonthica.* Using a previously published AFLP-derived marker that is specific to detect isolates of *F. oxysporum f.sp. strigae*, an effective soil-borne biocontrol agent against *Striga*, we also detected the gene in several other *Fusarium* species. As these isolates were all associated with the *Striga/Sorghum* pathosystem, the possibility of horizontal gene transfer among these fusaria will be of interest to further investigate in future.

Citation: Lombard L, van Doorn R, Groenewald JZ, Tessema T, Kuramae EE, Etolo DW, Raaijmakers JM, Crous PW (2022). *Fusarium* diversity associated with the *Sorghum-Striga* interaction in Ethiopia. *Fungal Systematics and Evolution* **10**: 177–215. doi: 10.3114/fuse.2022.10.08
Received: 1 September 2022; **Accepted:** 30 November 2022; **Effectively published online:** 5 December 2022
Corresponding editor: L. Cai

INTRODUCTION

Root parasitic weeds (RPWs) of the genera *Orobanche*, *Phelipanche* and *Striga* are major yield-limiting factors of a wide range of cereal crops such as maize, rice, millet, sorghum and the legume cowpea, particularly in Sub-Saharan Africa, India and Southeast Asia (Masteling *et al.* 2019). In sub-Saharan Africa, *Sorghum* production is seriously threatened by *Striga hermonthica* and *Striga asiatica*. *Striga* species are obligate hemiparasitic root parasites which penetrate the roots of host plants and absorb nutrients using a specialised organ known as haustoria. These RPWs have been estimated to infest some 64 % of the total cereal production area in West Africa (Gressel *et al.* 2004, Ejeta 2007, Parker 2012), and this figure is still increasing. For *Striga hermonthica* it has been estimated that 50–300 M ha (approximately equivalent to the size of France and India) of field soils in Africa are currently infested (Vurro *et al.* 2019). Crop infections can lead to grain yield losses of 20–80 % in Africa, but total crop losses have also been reported (Gurney *et al.* 2002).

Seed germination of obligate RPWs reply on host-derived signals released by the roots (*e.g.* strigolactones). Seed germination is followed by haustorium formation, leading to root infection. Other stages of the life cycle that are possible targets for disease control include the *Striga* soil seed bank, and seed production. Present control strategies include resistance breeding, hand weeding, alternative cropping practices, and chemical control (Eteja 2007). Because these strategies are only effective if applied in combination, an integrated systems approach is needed to provide effective and sustainable control of RWPs (Masteling *et al*. 2019).

Striga control depends on eliminating its seed reserves in soil (Daffalla *et al.* 2014). Species of the common soil-borne genus *Fusarium,* which have been isolated from diseased *Striga hermonthica* have proven to be highly pathogenic to all developmental stages of the parasite, including seeds. Some species are highly host-specific and non-pathogenic to a wide range of crops tested, thus rendering them as candidates to be used as mycoherbicides (Kroschel *et al.* 1999). Anteyi *et al.* (2022) reported that an isolate of *F. venenatum* produced the

exometabolite diacetoxyscirpenol (DAS), which consistently inhibited seed germination of diverse *S. hermonthica* seedlots. Furthermore, surveys for fungal pathogens of *Striga* spp. revealed that *Fusarium* species (especially *F. oxysporum*) were the most prominent pathogens associated with diseased *Striga* spp. (Sauerborn *et al.* 2007), with several species showing significant disease development in this host when tested under controlled and/or field conditions (Abbasher & Sauerborn 1992, Ciotola *et al.* 1995, 2000, Abbasher *et al.* 1996, Kroschel *et al.* 1996, Sauerborn *et al.* 1996a, 2007, Hess *et al.* 2002, Marley *et al.* 2004). In such trials the application of isolates of *F. nygamai* and *F. oxysporum* caused more than 90 % reduction of *S. hermonthica* emergence (Abbasher & Sauerborn, 1992, Ciotola *et al.* 1995). Furthermore, isolates of *F. oxysporum* f.sp. *strigae* (Abbasher *et al.* 1995, Marley *et al.* 1999) resulted in a positive result when it was used as a biological control agent against *Striga* (Abbasher *et al.* 1995, Ciotola *et al.* 1995, Kroschel *et al.* 1996, Marley *et al.* 1999). It has also been shown that *F. incarnatum* greatly reduced the germination, survival and attachment of *S. asiatica* on maize roots (Abbasher *et al.* 1996).

Based on these findings, the aim of the present study was to determine which *Fusarium* species are commonly associated with *Sorghum* and rhizosphere soils, or as endophytes with *Sorghum* roots and seeds, or *Striga* stems and seeds.

MATERIALS AND METHODS

Isolates

Soil

Soil samples with varying levels of *Striga* infestation were collected in Ethiopia (samples E1–E47). To collect sorghum rhizophere-associated fungi, cultivar Teshale was grown in pots containing the 47 soils under greenhouse conditions and the rhizosphere suspension was collected from 5-wk-old plants. Fungal isolations followed the methods of Groenewald *et al.* (2018) and Giraldo *et al*. (2019). Colonies were sub-cultured on 2 % potato dextrose agar (PDA), oatmeal agar (OA), malt extract agar (MEA) (Crous *et al*. 2019), synthetic nutrient-poor agar (SNA; Nirenberg 1976), carnation leaf agar (CLA; Fisher *et al*. 1982), and incubated at 25 °C under continuous near-ultraviolet light to promote sporulation. Reference isolates and specimens of the studied *Fusarium* spp. are maintained in the Ethiopian Biodiversity Institute (EBI), Addis Ababa, Ethiopia (EMCC-F) and in the working collection of Lorenzo Lombard, housed at the Westerdijk Fungal Biodiversity Institute, Utrecht, The Netherlands (LLC).

Endophytes

Fungal endophytes were isolated from 53 *Striga* plant stems, 107 *Sorghum* roots and root collars, from 20 seeds from each of 59 different *Sorghum* genotypes, and from seeds of *Striga asiatica* collected in Derashe and from *S. hermonthica* collected in Abergelle, Asosa, Feddis, Humera, Kobo, with 150 seeds per sample.

Plant stems and roots were washed with running tap water, and 5-mm segments were cut with a sterilised scalpel, and immersed into the following series of solutions: sterile distilled H_2O for 60 s, 70 % ethanol for 60 s, 2.5 % sodium hypochlorite for 4 min, 70 % ethanol for 30 s, and a final rinse in sterile distilled H_2O. *Striga* and *Sorghum* seeds were treated in a similar fashion, except that they were rinsed for longer in 2.5 % sodium hypochlorite (5 min), and afterwards the seedcoat was broken with a pincette. All tissues were plated onto malt extract agar with antibiotics (Penicillin-Streptomycin), to inhibit bacterial growth and incubated on a laboratory bench (21 °C). Plates were checked daily for fungal growth, and emerging colonies were hyphal tipped, re-inoculated on fresh MEA plates, and colonised agar plugs maintained at -80 °C in 10 % (v/v) glycerol (Crous *et al*. 2019).

DNA extraction, amplification (PCR), phylogeny and AFLP-based marker testing

Protocols for genomic DNA isolation, PCR amplification of partial calmodulin (*CaM*) gene, DNA-directed RNA polymerase II largest (*rpb1*) and second largest subunit (*rpb2*) genes, and translation elongation factor 1-alpha (*tef1*) gene, and sequencing of the novel isolates (Supplementary Table S1) followed Crous *et al.* (2021b). Sequences derived in this study were deposited in GenBank (Supplementary Table S1), the alignments and phylogenetic trees in figshare (doi: 10.6084/m9.figshare.21080776).

Initial identifications to species complex level were made using megablast searches (Zhang *et al*. 2000) of the obtained sequences against NCBIs GenBank nucleotide database and the Fusarioid-ID database (www.fusarium.org; Crous *et al.* 2021b). Reference sequences (Supplementary Table S2) and based on megablast searches were then used to construct single-gene and multi-gene alignments for the different *Fusarium* species complexes. Phylogenetic analyses using RAxML v. 8.0.0 (Stamatakis 2014), IQ-TREE v. 2.1.3 (Nguyen *et al*. 2015, Minh *et al*. 2020) and MrBayes v. 3.2.7 (Ronquist & Huelsenbeck 2003) followed Crous *et al.* (2021b), with the exception that trees were saved every 10 or 100 generations (Supplementary Table S3). All resulting trees were printed with Geneious Prime v. 2022.1.1 (Biomatters Ltd, Auckland, New Zealand) and the layout of the trees was done in Adobe Illustrator v. CC 2021.

The absence or presence of an explicit AFLP-based marker associated with *Fusarium oxysporum f.sp. strigae* (Fos) was also tested for all novel isolates (Supplementary Table S1). DNA amplification conditions and primers follow Zimmermann *et al.* (2015). Sanger sequencing was performed on all positive amplicons and compared to the reference sequence provided by Zimmermann *et al.* (2015) to confirm that the correct gene fragment was obtained.

Morphology

Slide preparations were mounted in water, from colonies sporulating on CLA, following the protocols described by Crous *et al*. (2021b). Observations were made with a Nikon SMZ25 dissection microscope, and with a Zeiss Axio Imager 2 light microscope using differential interference contrast (DIC) illumination and images recorded on a Nikon DS-Ri2 camera with associated software. Colony characters and pigment production were noted after 7 d of growth on MEA, PDA and OA incubated at 25 °C. Colony colours (surface and reverse) were scored using the colour charts of Rayner (1970). Taxonomic novelties were deposited in MycoBank (www.MycoBank.org; Crous *et al*. 2004).

RESULTS

Isolates

In the present study, 439 isolates representing 42 species (including two as "*Fusarium* sp." and three novel species) from eight species complexes were obtained from the abovementioned substrates (Supplementary Table S1). These are treated below in the Taxonomy section.

Phylogeny

Four multigene alignments were generated in the present study and subjected to the three phylogenetic analyses described above. Statistical values for the alignments and phylogenetic trees are summarised in Supplementary Table S3.

Fusarium burgessii, *F. concolor* and *F. incarnatum* species complexes (Fig. 1): Isolates clustered with 10 known species, and two novel lineages which are formally named below. Known species are *F. concolor* (FCOSC), *F. burgessii* (FburSC) and *F. caatingaense*, *F. clavus*, *F. compactum*, *F. duofalcatisporum*, *F. incarnatum*, *F. lacertarum*, *F. nanum* and *F. serpentinum* (FIESC). The two novel species, *F. extenuatum* and *F. tangerinum*, belong to the FIESC. The three phylogenetic analyses (RAxML, IQ-TREE and MrBayes) overall displayed the same species clades and mainly differed with regards to the backbone relationships between species clades/lineages (data not shown, support and posterior probability values are superimposed on the presented figure).

Fusarium chlamydosporum, *F. sambucinum* and *F. tricinctum* species complexes (Fig. 2): Novel isolates clustered with six known species, and one novel lineage (previously called *Fusarium* sp. FSAMSC 28) which are formally named below. Known species are *F. avenaceum* (FTSC), *F. nelsonii* and *F. sporodochiale* (FCSC) and *F. brachygibbosum*, *F. subflagellisporum* and *F. transvaalense* (FSAMSC). The novel species, *F. pentaseptatum*, belongs to the FSAMSC. The three phylogenetic analyses (RAxML, IQ-TREE and MrBayes) overall displayed the same species clades and mainly differed with regards to the backbone relationships between species clades/lineages (data not shown, support and posterior probability values are superimposed on the presented figure).

Fusarium fujikuroi species complex (Fig. 3): Novel isolates represent one undescribed species and clustered with 14 known species, namely *F. andiyazi*, *F. annulatum*, *F. brevicatenulatum*, *F. caapi*, *F. ficicrescens*, *F. fredkrugeri*, *F. lactis*, *F. mirum*, *F. nygamai*, *F. secorum*, *F. sudanense*, *F. thapsinum*, *F. udum* and *F. verticillioides*. The three phylogenetic analyses (RAxML, IQ-TREE and MrBayes) overall displayed the same species clades and mainly differed with regards to the backbone relationships between species clades/lineages (data not shown, support and posterior probability values are superimposed on the presented figure).

Fusarium oxysporum species complex (Fig. 4): Novel isolates clustered with seven known species, namely *F. curvatum*, *F. fabacearum*, *F. glycines*, *F. gossypinum*, *F. libertatis*, *F. odoratissimum* and *F. veterinarium*, as well as one species clade which was labelled as "*Fusarium* sp. 1" by Crous *et al*. (2021a). The three phylogenetic analyses (RAxML, IQ-TREE and MrBayes) overall displayed the same species clades and mainly differed with regard to the backbone relationships between species clades/lineages (data not shown, support and posterior probability values are superimposed on the presented figure).

Based on these phylogenetic trees, several taxonomic decisions were made, and the individual and combined trees are discussed under the Notes in the Taxonomy section below, where applicable.

AFLP-based marker for Fos

DNA of all 439 isolates obtained in this study were subjected to a PCR amplification of the AFLP-based marker for Fos, resulting in 66 amplicons (Supplementary Table S1). Sequence analyses of these amplicons revealed that most of the sequences (49 isolates) match the reference sequence from Zimmermann *et al.* (2015) (labelled here as haplotype 1a). However, six other sequence haplotypes are also observed (Fig. 5). Two of these differ by one and two substitutions from the reference sequence, respectively (haplotypes 1b and 1c; one isolate each). Although haplotype 2 (one isolate) differs with 7 substitutions from the reference sequence. These differences could be derived from haplotype 4a, and could be indicative of recombination events between haplotypes 1a and 4a. Haplotype 3 (two isolates) also appears to be an intermediate form between haplotypes 1a and 4a but has five unique substitutions not present in any of the other haplotypes. There are 19 substitutions between haplotypes 1a and 4a (11 isolates), with haplotype 4b (one isolate) appearing to be an additional intermediate form between haplotypes 1a and 4a.

The AFLP-based marker for Fos is quite prevalent in the *Fusarium oxysporum* species complex (FOSC) (32 amplicons out of 60 isolates tested) and FSAMSC (17 amplicons out of 44 isolates tested). A single isolate out of the four *Fusarium chlamydosporum* species complex (FCSC) isolates is positive but given the low number of isolates tested, this value should not be considered significant until more isolates are tested. The two remaining species complexes, *Fusarium fujikuroi* species complex (FFSC) and *Fusarium incarnatum/equiseti* species complex (FIESC), only have 11 and 5 amplicons out of 230 and 99 isolates tested, respectively (Fig. 6). Haplotype 1a is present and the dominant haplotype in all of the species complexes, except for the *Fusarium sambucinum* species complex (FSAMSC) complex where haplotype 4a is the dominant haplotype (Fig. 6). None of the isolates from *Fusarium burgessii* species complex (FburSC) or *Fusarium concolor* species complex (FconSC) tested positive (Fig. 7).

Haplotype 1a is present in all species that amplified for the AFLP-based marker for Fos, except for *F. subflagellisporum* (FSAMSC) which mainly contains haplotype 4a and haplotypes 1b and 3 to a much lesser extent (Fig. 7). *Fusarium fabacearum* and *F. veterinarium* (both FOSC) contain the largest number of amplicons of haplotype 1a, with the haplotype being present in almost all *F. veterinarium* isolates tested and in roughly half of the *F. fabacearum* isolates tested (Fig. 7). The AFLP-based marker for Fos amplified in more than half of the *F. subflagellisporum* (FSAMSC) isolates, but sequence analyses of these amplicons revealed the dominant haplotype to be haplotype 4a (Fig. 7).

Taxonomy

Based on the results obtained, 42 *Fusarium* species were identified, including three species which are newly described below. Collection details of the material examined can be found in Supplementary Table S1.

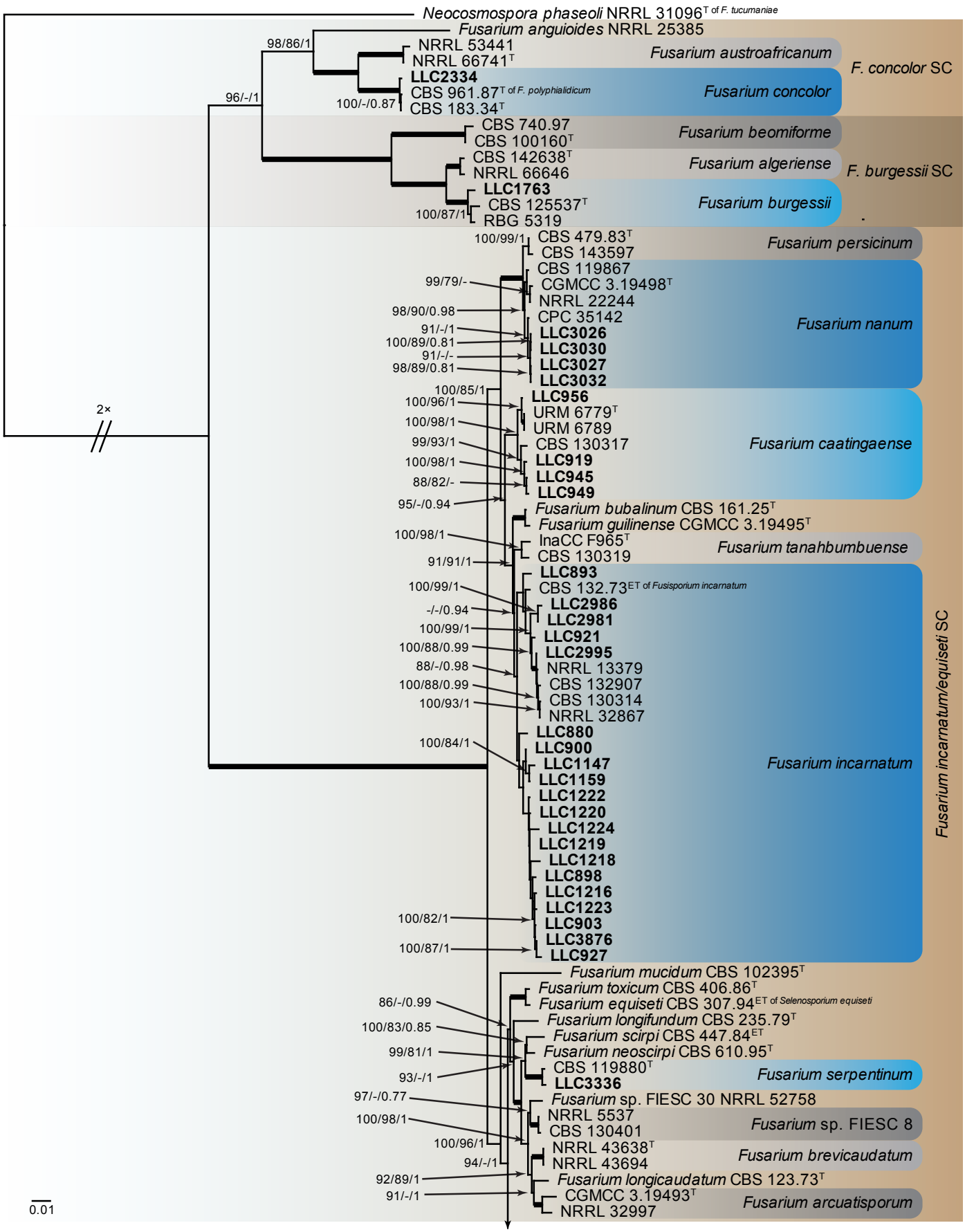

Fig 1. The IQ-TREE maximum likelihood consensus tree inferred from the combined *CaM*, *rpb1*, *rpb2* and *tef1* sequence alignment. Thickened lines indicate nodes with full support (RAxML & IQ-TREE bootstrap = 100 %; PP = 1.0) with support values of other nodes indicated at the branches (IQ-TREE > 84 % / RAxML > 74 % / PP > 0.74). The tree is rooted to *Neocosmospora phaseoli* (NRRL 31096, ex-type culture). The scale bar indicates the number of expected changes per site. Species complexes are indicated on the right and highlighted with coloured blocks (brown tints). Species clades containing the novel isolates (in bold) are highlighted with coloured blocks (blue tints). Additional species clades are shown in coloured blocks with grey tints. Taxonomic novelties recognised in this study are shown in bold text.

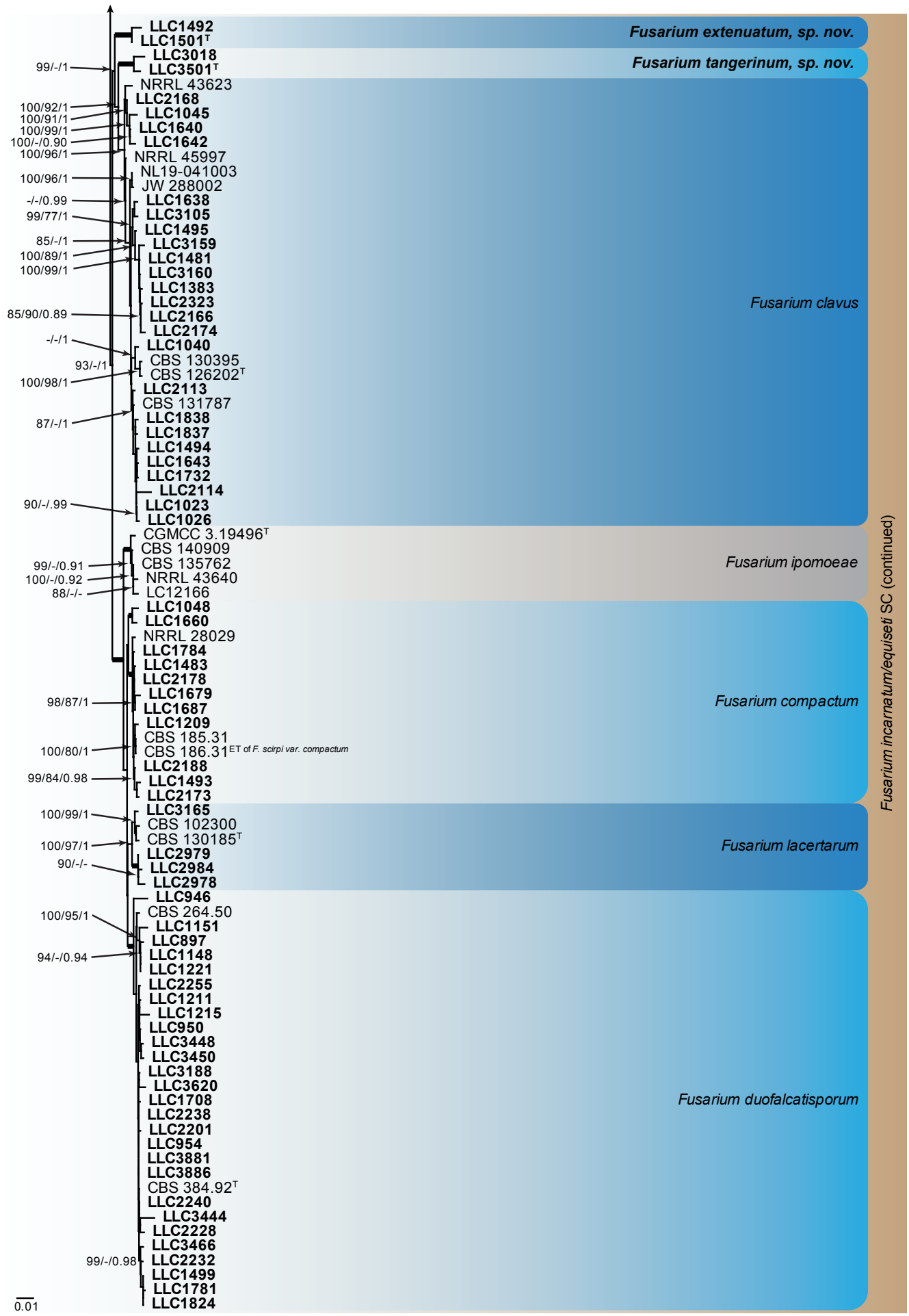

Fig 1. (Continued).

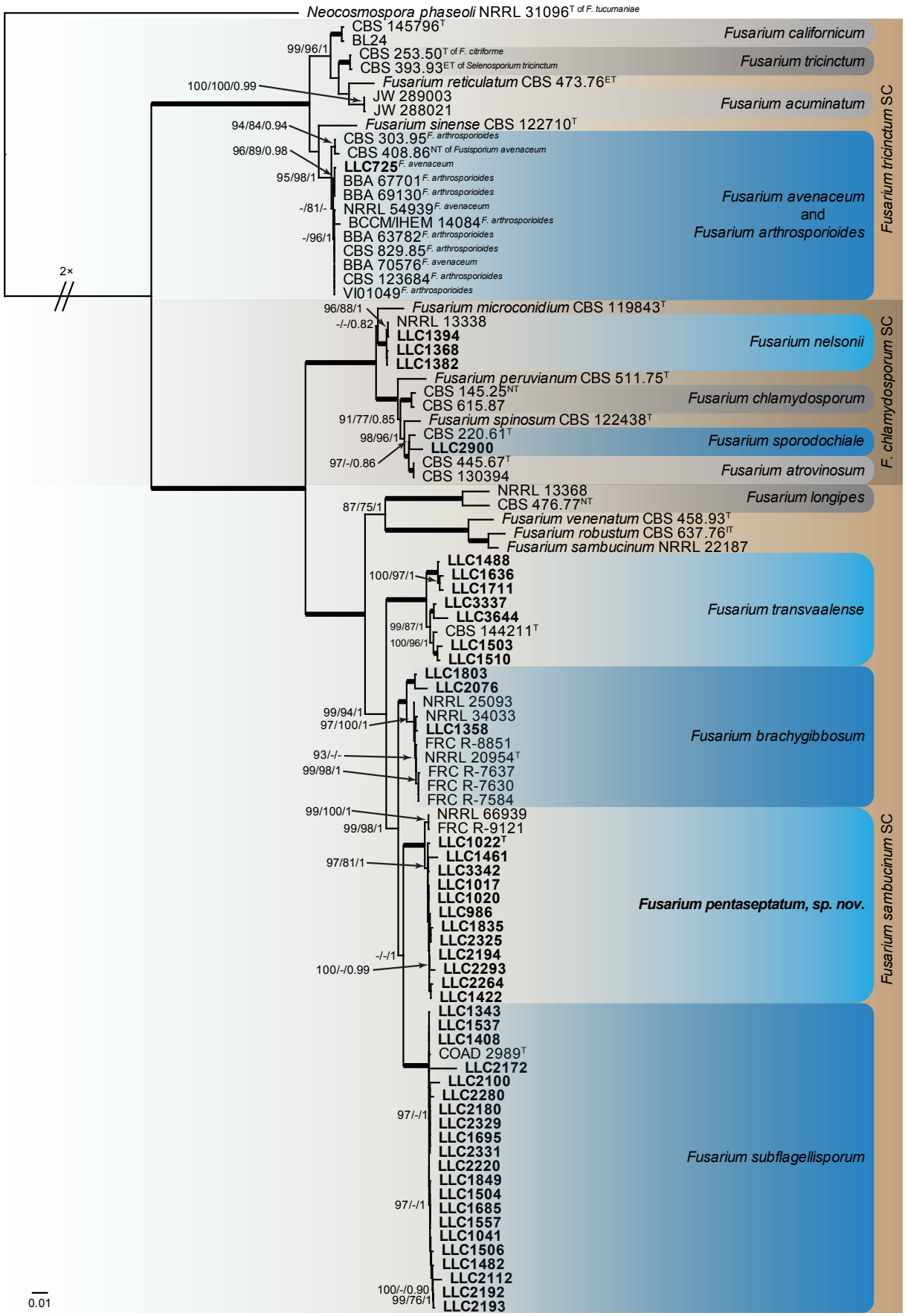

Fig 2. The IQ-TREE maximum likelihood consensus tree inferred from the combined *CaM*, *rpb1*, *rpb2* and *tef1* sequence alignment. Thickened lines indicate nodes with full support (RAxML & IQ-TREE bootstrap = 100 %; PP = 1.0) with support values of other nodes indicated at the branches (IQ-TREE > 84 % / RAxML > 74 % / PP > 0.74). The tree is rooted to *Neocosmospora phaseoli* (NRRL 31096, ex-type culture). The scale bar indicates the number of expected changes per site. Species complexes are indicated on the right and highlighted with coloured blocks (brown tints). Species clades containing the novel isolates (in bold) are highlighted with coloured blocks (blue tints). Additional species clades are shown in coloured blocks with grey tints. The taxonomic novelty recognised in this study is shown in bold text.

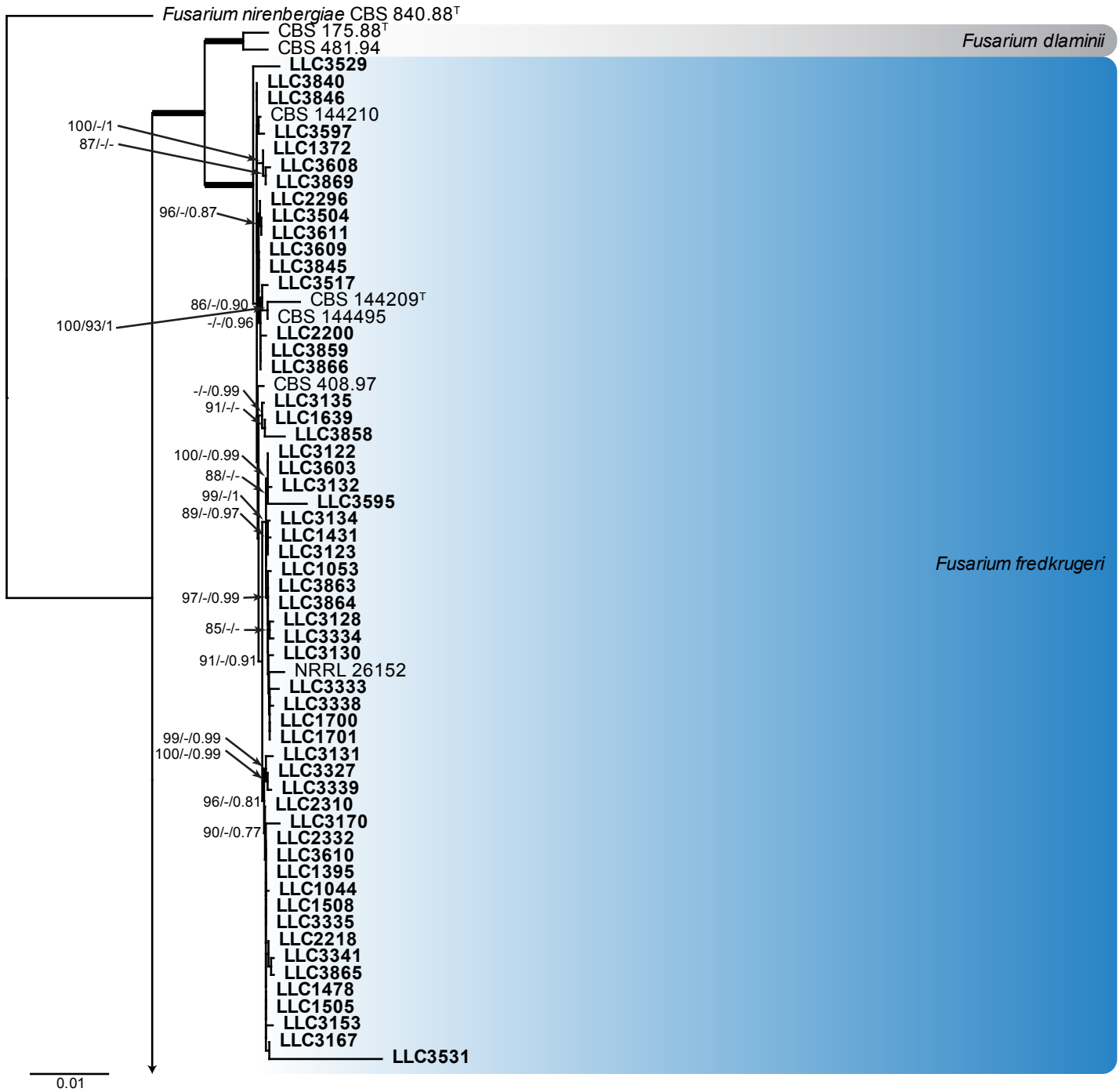

Fig 3. The IQ-TREE maximum likelihood consensus tree inferred from the combined *CaM*, *rpb1*, *rpb2* and *tef1* sequence alignment. Thickened lines indicate nodes with full support (RAxML & IQ-TREE bootstrap = 100 %; PP = 1.0) with support values of other nodes indicated at the branches (IQ-TREE > 84 % / RAxML > 74 % / PP > 0.74). The tree is rooted to *Fusarium nirenbergiae* (CBS 840.88, ex-type culture). The scale bar indicates the number of expected changes per site. Species clades containing the novel isolates (in bold) are highlighted with coloured blocks (blue tints). Additional species clades are shown in coloured blocks with grey tints.

Fusarium burgessii species complex (FburSC)

Fusarium burgessii M.H. Laurence *et al.*, *Fungal Diversity* **49**: 109. 2011.

Materials examined: Supplementary Table S1.

Notes: Isolate LLC1763 clusters with the ex-type and additional isolate of *F. burgessii* with full support (Fig. 1, part 1).

Fusarium chlamydosporum species complex (FCSC)

Fusarium sporodochiale L. Lombard & Crous, *Fungal Syst. Evol.* **4**: 196. 2019.

Materials examined: Supplementary Table S1.

Notes: Isolate LLC2900 (Fig. 2) is a sister lineage to *F. sporodochiale* with low support (IQ-TREE bootstrap = 97 % / RAxML bootstrap = <74 % / PP = 0.86). The *CaM* sequence of isolate LLC2900 is 98.87 % (524/530 nt) identical to the ex-type

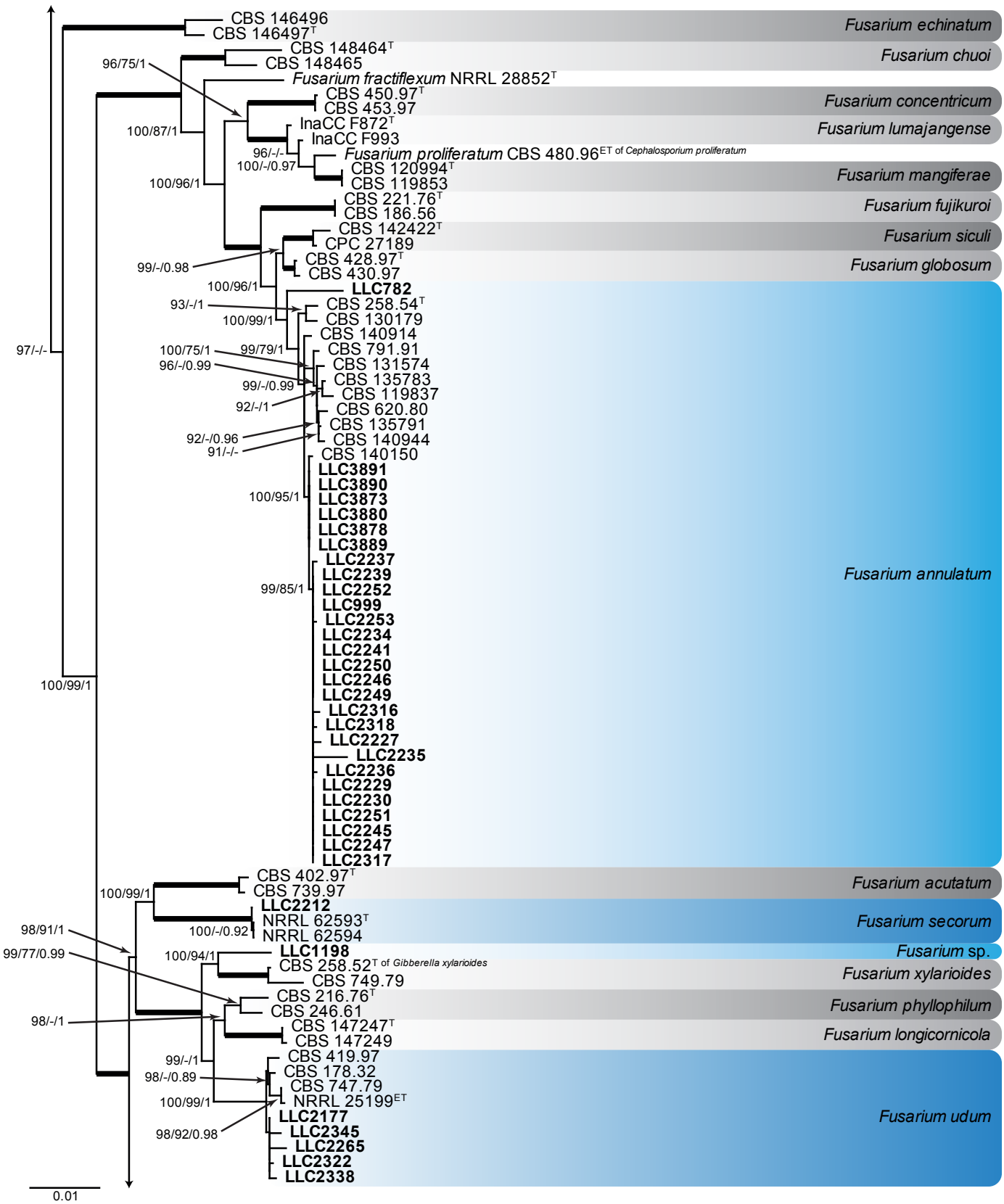

Fig 3. (Continued).

isolate of *F. sporodochiale* (CBS 220.61), the *rpb1* sequence 98.57 % (827/839 nt), the *rpb2* sequence 99.89 % (873/874 nt), and the *tef1* sequence 98.84 % (681/689 nt).

Fusarium nelsonii Marasas & Logrieco, *Mycologia* **90**: 508. 1998.

Materials examined: Supplementary Table S1.

Notes: The isolates cluster with *F. nelsonii* isolate NRRL 13338 with full support (Fig. 2).

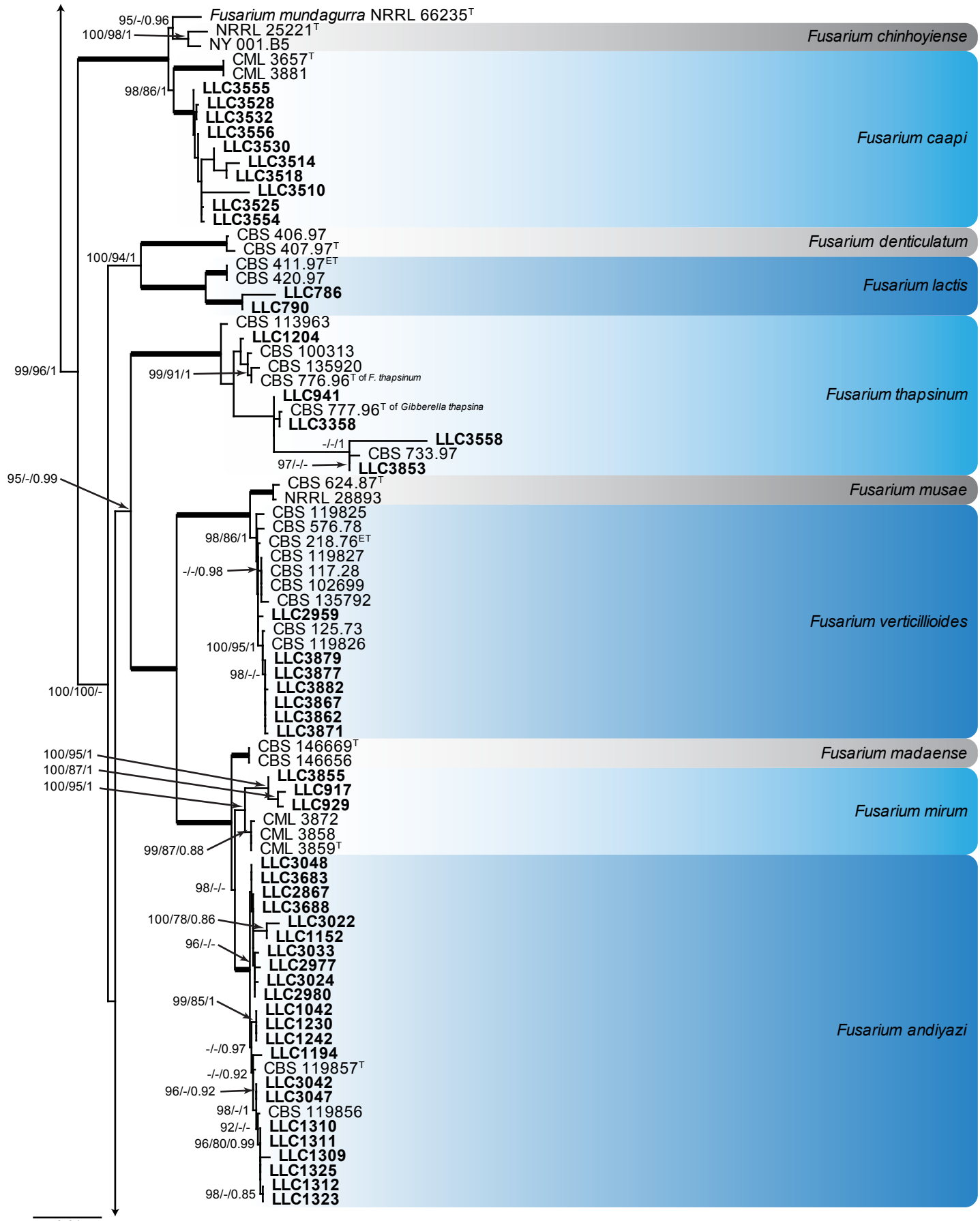

Fig 3. (Continued).

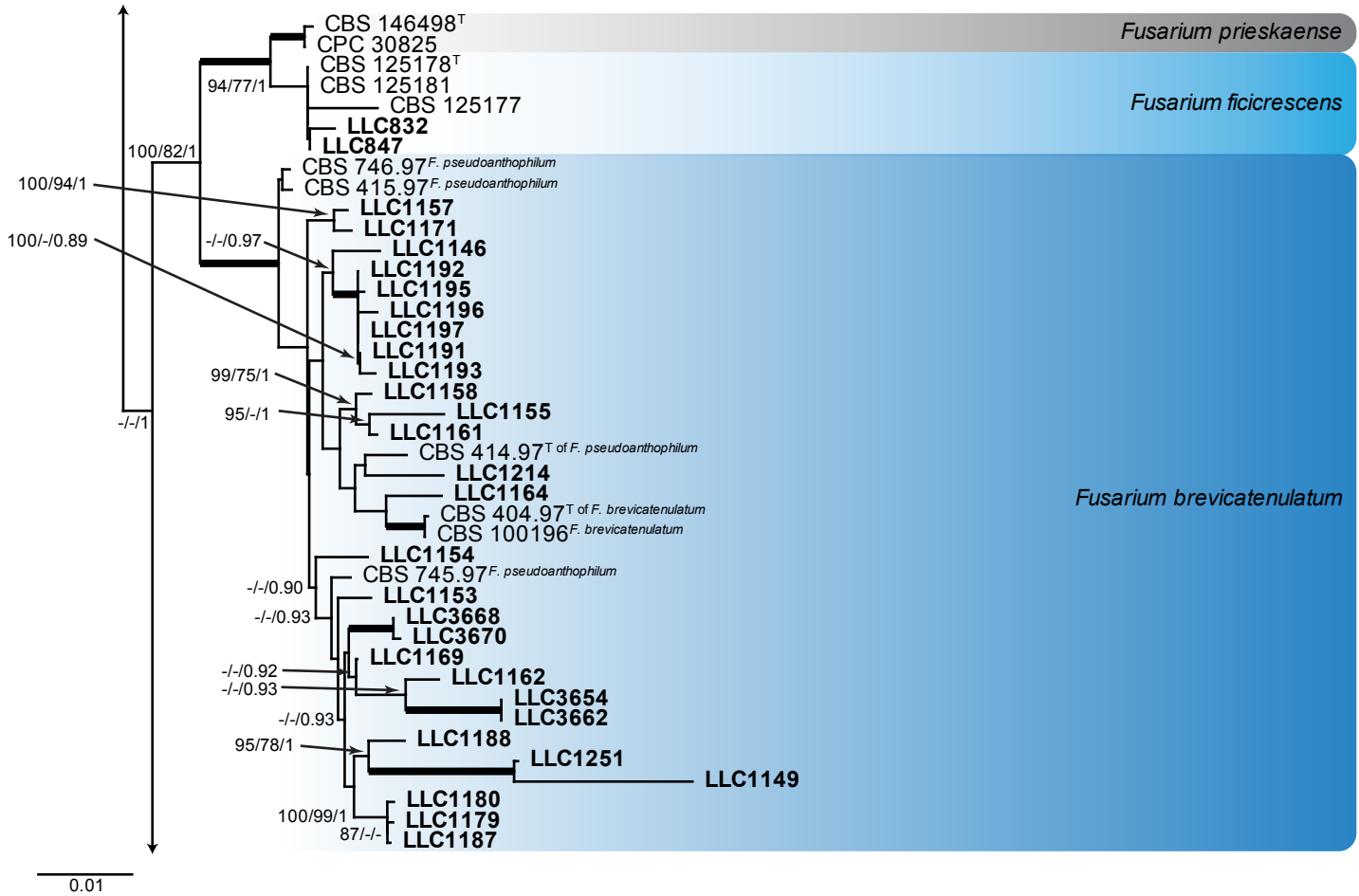

Fig 3. (Continued).

Fusarium concolor species complex (FCOSC)

Fusarium concolor Reinking, *Centbl. Bakt. ParasitKde*, Abt. II **89**: 512. 1934.
Synonym: *Fusarium polyphialidicum* Marasas *et al.*, *Mycologia* **78**: 678. 1986.

Materials examined: Supplementary Table S1.

Note: Isolate LLC2334 clusters with the ex-types of *F. concolor* and *F. polyphialidicum* with full support (Fig. 1, part 1).

Fusarium fujikuroi species complex (FFSC)

Fusarium andiyazi Marasas *et al.*, *Mycologia* **93**: 1205. 2001.

Materials examined: Supplementary Table S1.

Notes: The isolates cluster with the ex-type of *F. andiyazi* with full support (Fig. 3, part 3). Although there is some genetic variation, the internal structure of the species is poorly supported.

Fusarium annulatum Bugnic., *Rev. Gén. Bot.* **59**: 17. 1952. Fig. 8.

Materials examined: Supplementary Table S1.

Notes: *Fusarium annulatum* LLC782 (Fig. 3, part 2) clusters basal to the *F. annulatum* clade. The *F. annulatum s. str.* subclade containing the ex-type isolate is moderately supported (IQ-TREE bootstrap = 99 % / RAxML bootstrap = 79 % / PP = 1) whereas the association between LLC782 and *F. annulatum s.str.* was highly supported (IQ-TREE bootstrap = 100 % / RAxML bootstrap = 99 % / PP = 1). No *CaM* or *rpb1* sequence of isolate LLC782 was available for comparison. The *rpb2* sequence of isolate LLC782 is 98.86 % (954/965 nt) identical to the ex-type isolate of *F. annulatum* (CBS 258.54), and the *tef1* sequence 98.52 % (665/675 nt). As we were unable to generate *CaM* and *rpb1* sequence data for this isolate, the sequence similarity to *F. annulatum* is quite high, and *F. annulatum* is already genetically quite variable, we refrain from introducing a novel species for this this isolate.

Fusarium brevicatenulatum Nirenberg *et al.*, *Mycologia* **90**: 460. 1998.
Synonym: *Fusarium pseudoanthophilum* Nirenberg *et al.*, *Mycologia* **90**: 461. 1998.

Materials examined: Supplementary Table S1.

Notes: The isolates cluster with the ex-types of *F. brevicatenulatum* and *F. pseudoanthophilum* with full support (Fig. 3, part 4). Although there is quite a bit of genetic variation in the species clade, the internal structure of the species is poorly supported. The present study expands the sampling for these two species published by Yilmaz *et al*. (2021; names from that publication shown in superscript). Based on this broader sampling and genetic diversity, we follow the suspicion of Leslie & Summerell (2006), and synonymise *F. pseudoanthophilum* under *F. brevicatenulatum*.

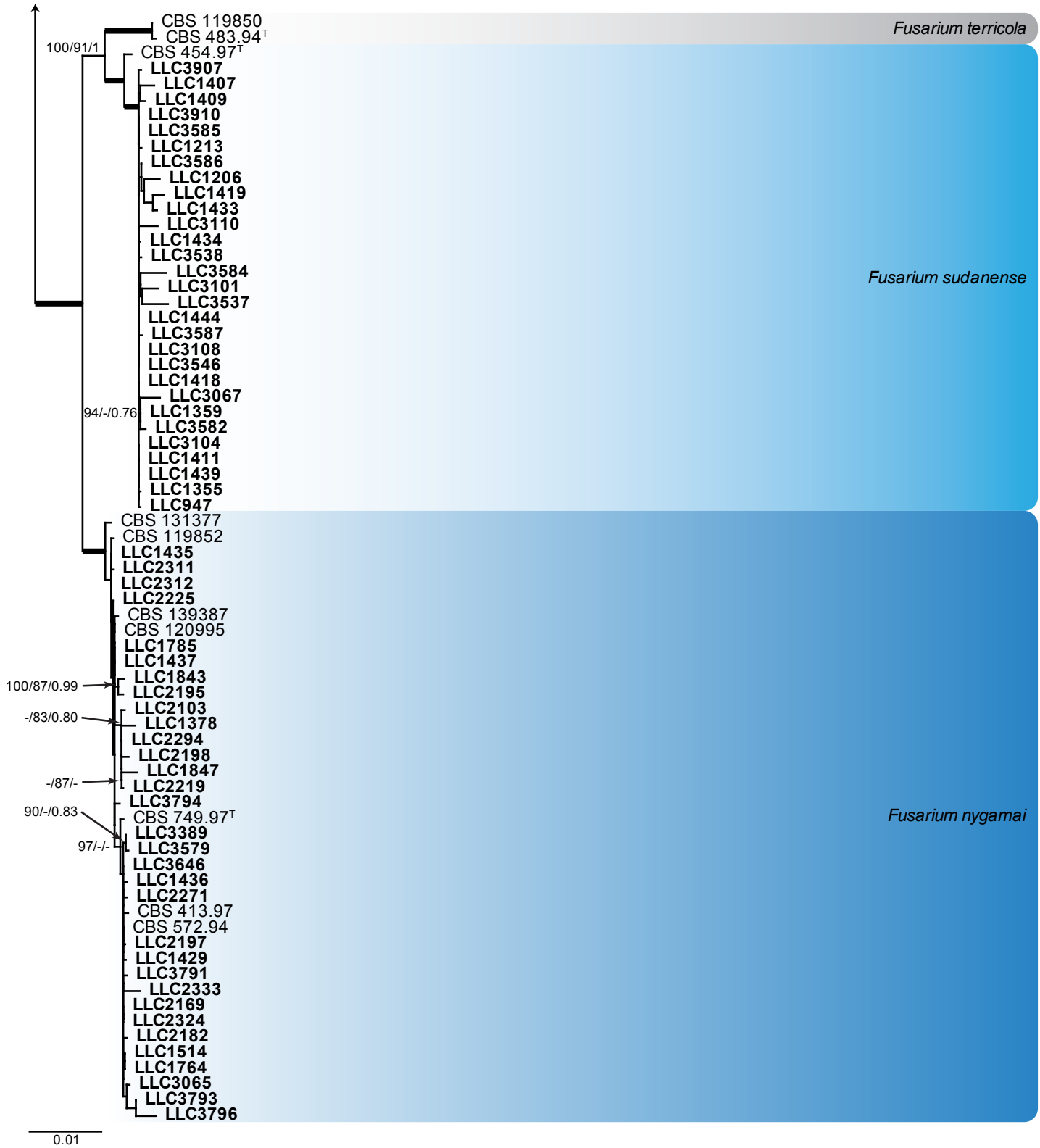

Fig 3. (Continued).

Fusarium caapi M.M. Costa *et al.*, *Mycol. Progr.* **20**: 67. 2021. Fig. 9.

Materials examined: Supplementary Table S1.

Notes: The *CaM* sequence of isolate LLC3528 is 99.67% (608/610 nt) and 99.02% (606/612 nt) identical to the ex-type isolates of *F. chinhoyiense* (NRRL 25221) and *F. mundagurra* (NRRL 66235), respectively (Fig. 3, part 3). No *CaM* sequence is available for *F. caapi* (CML 3657). The *rpb1* sequence of isolate LLC3528 is 99.46 % (741/745 nt) and 99.72 % (723/725 nt) identical to the ex-type isolates of *F. chinhoyiense* (NRRL 25221) and *F. mundagurra* (NRRL 66235), respectively. No *rpb1* sequence is available for *F. caapi* (CML 3657). The *rpb2* sequence of isolate LLC3528 is 98.56 % (821/833 nt), 99.53 % (853/857 nt) and 99.14 % (806/813 nt) identical to the ex-type isolates of *F. caapi* (CML 3657), *F. chinhoyiense* (NRRL 25221) and *F. mundagurra* (NRRL 66235), respectively. The *tef1* sequence of isolate LLC3528 is 98.86 %

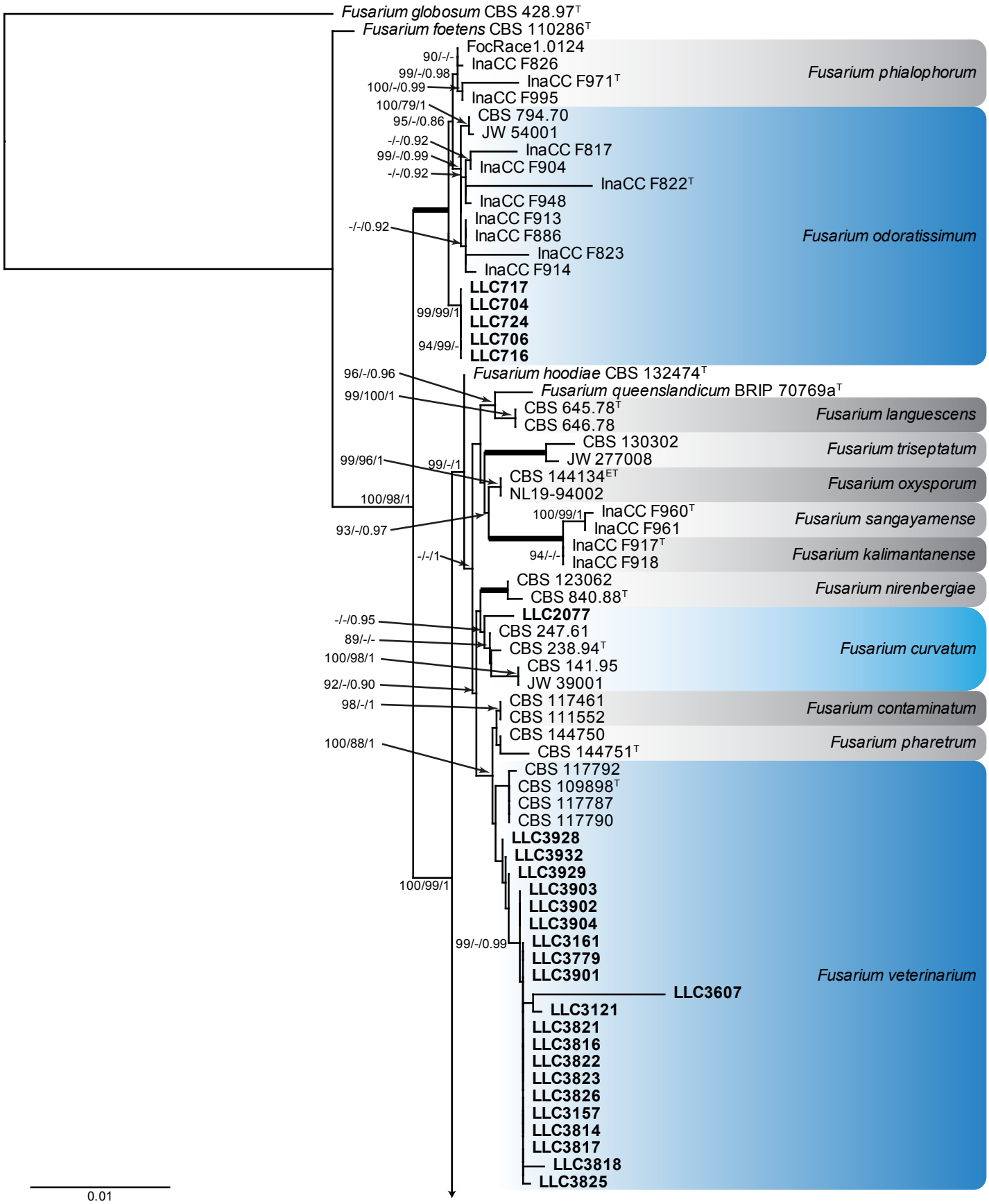

Fig 4. The IQ-TREE maximum likelihood consensus tree inferred from the combined *CaM*, *rpb1*, *rpb2* and *tef1* sequence alignment. Thickened lines indicate nodes with full support (RAxML & IQ-TREE bootstrap = 100 %; PP = 1.0) with support values of other nodes indicated at the branches (IQ-TREE > 84 % / RAxML > 74 % / PP > 0.74). The tree is rooted to *Fusarium globosum* (CBS 428.97, ex-type culture). The scale bar indicates the number of expected changes per site. Species clades containing the novel isolates (in bold) are highlighted with coloured blocks (blue tints). Additional species clades are shown in coloured blocks with grey tints.

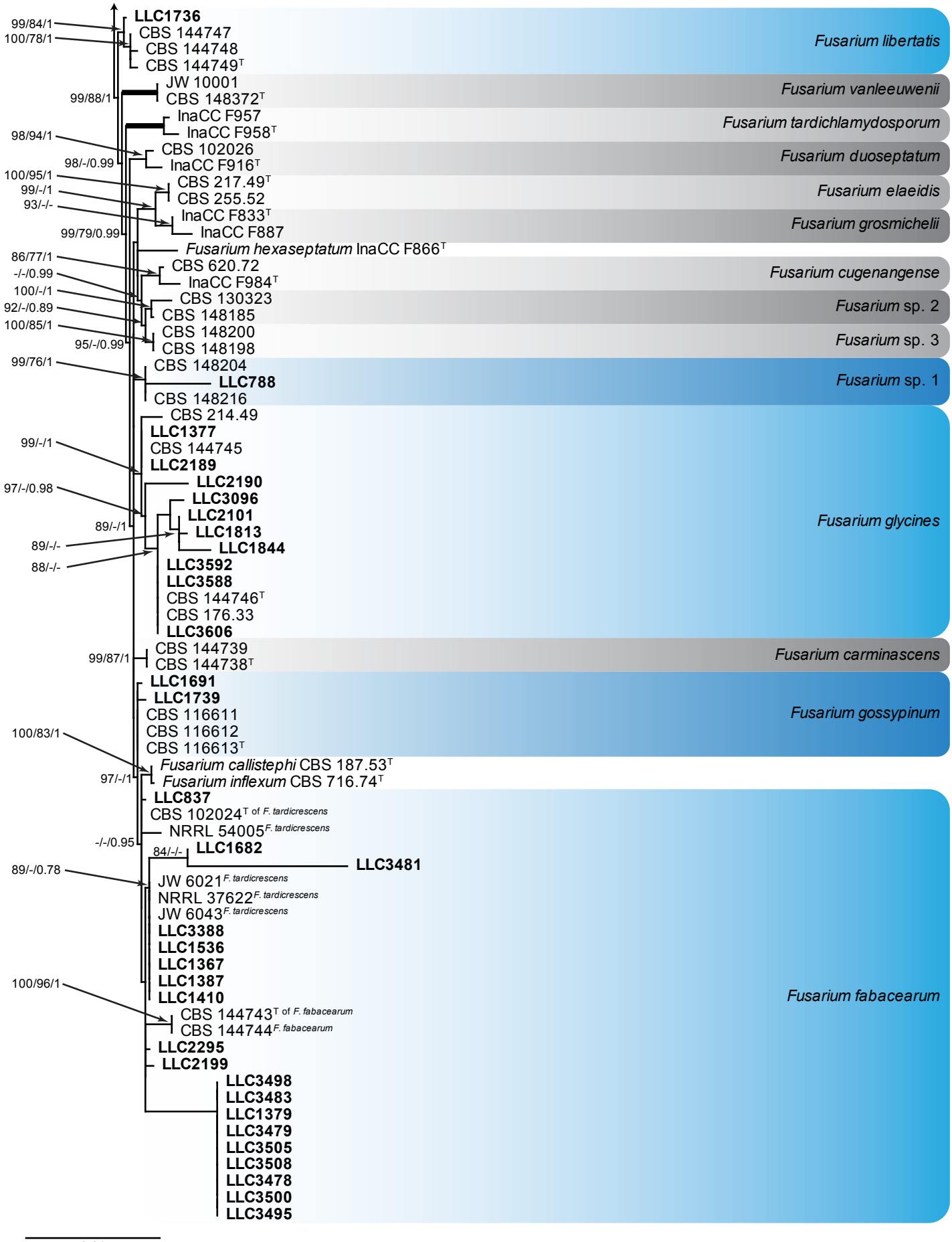

Fig 4. (Continued).

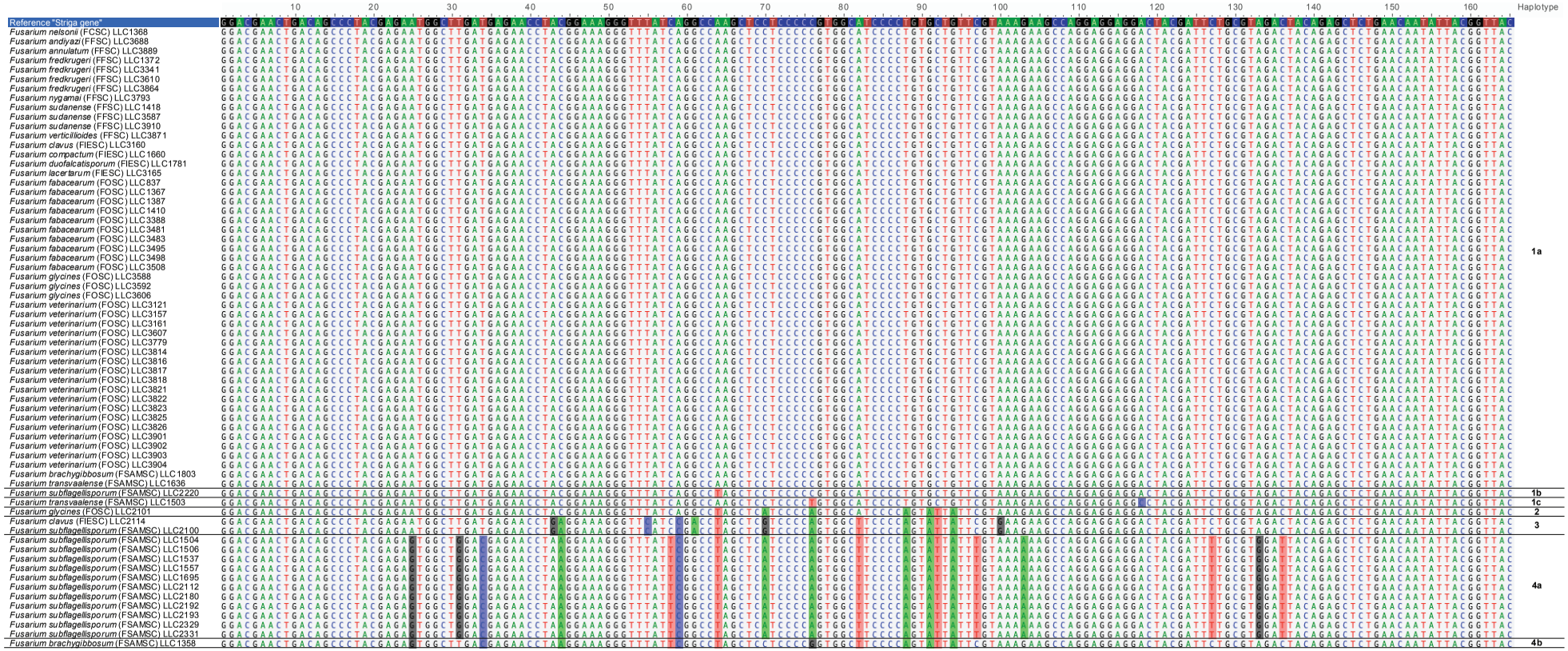

Fig. 5. Sequence alignment of sequences obtained for the *Striga* AFLP-derived marker amplicons with nucleotide substitutions compared to the reference sequence highlighted and haplotypes indicated to the right of the figure. Sequences in this figure were deposited in GenBank under accession numbers OP600320–OP600385.

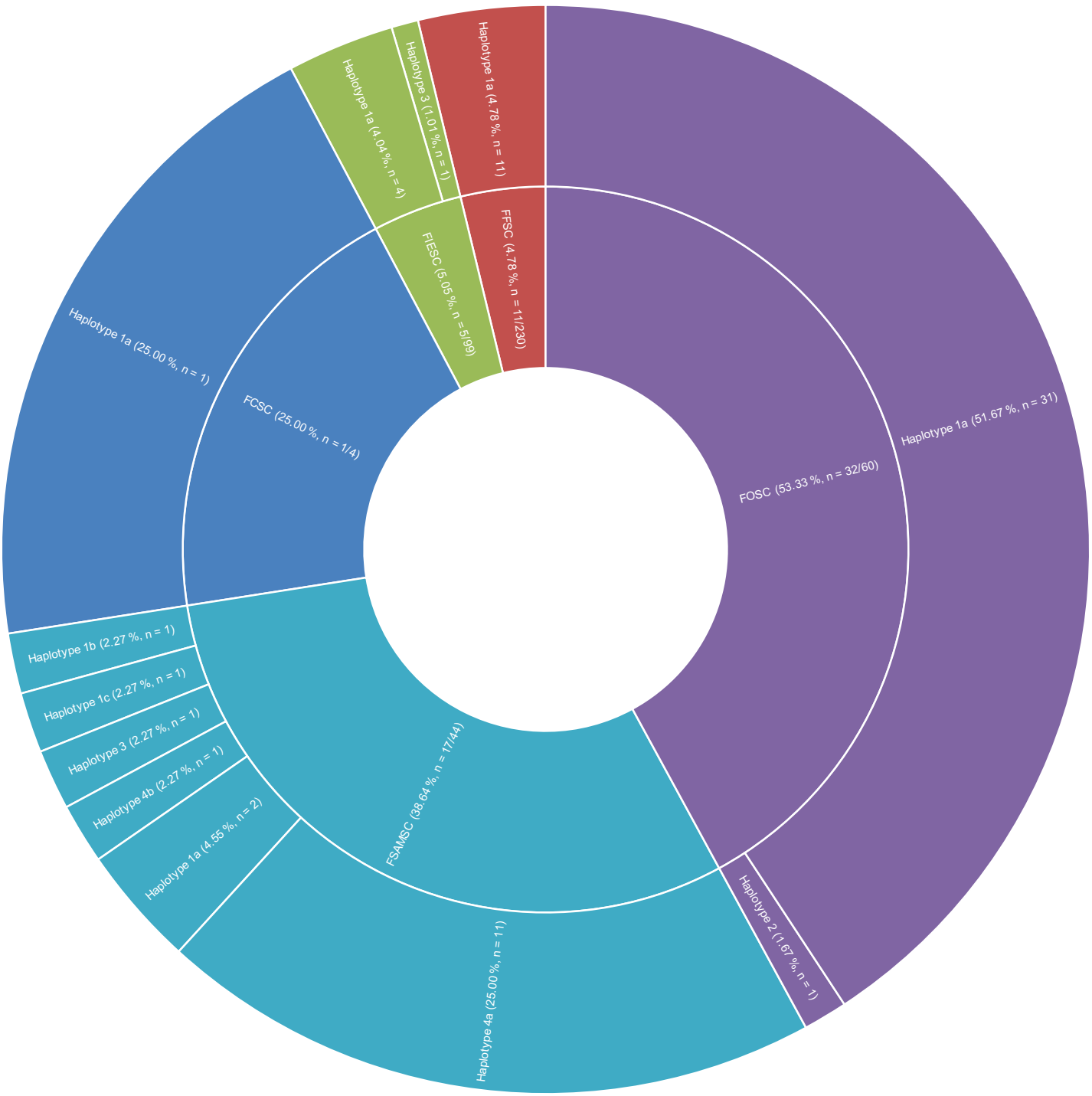

Fig. 6. Graph showing the distribution of haplotypes per species complex. The percentage is calculated per species complex from the number of positive tests divided by the total number of tests performed in the species complex. The pie part for the FCSC complex is artificially large due to being represented by only four isolates. FCSC: *Fusarium chlamydosporum* species complex; FFSC: *Fusarium fujikuroi* species complex; FIESC: *Fusarium incarnatum/equiseti* species complex; FOSC: *Fusarium oxysporum* species complex; FSAMSC: *Fusarium sambucinum* species complex.

(435/440 nt), 98.02 % (644/657 nt) and 98.35 % (537/546 nt) identical to the ex-type isolates of *F. caapi* (CML 3657), *F. chinhoyiense* (NRRL 25221) and *F. mundagurra* (NRRL 66235), respectively.

Fusarium ficicrescens Al-Hatmi *et al.*, *Fungal Biol.* **120**: 274. 2015.

Materials examined: Supplementary Table S1.

Notes: The two isolates cluster with the ex-type of *F. ficicrescens* with some to moderate support (IQ-TREE bootstrap = 94 % / RAxML bootstrap = 77 % / PP = 1; Fig. 3, part 4).

Fusarium fredkrugeri Sand.-Den. *et al.*, *MycoKeys* **34**: 79. 2018.

Materials examined: Supplementary Table S1.

Notes: The isolates cluster with the ex-type of *F. fredkrugeri* with full support (Fig. 3, part 1). Although there is some genetic variation in the species clade, the internal structure of the species is poorly supported.

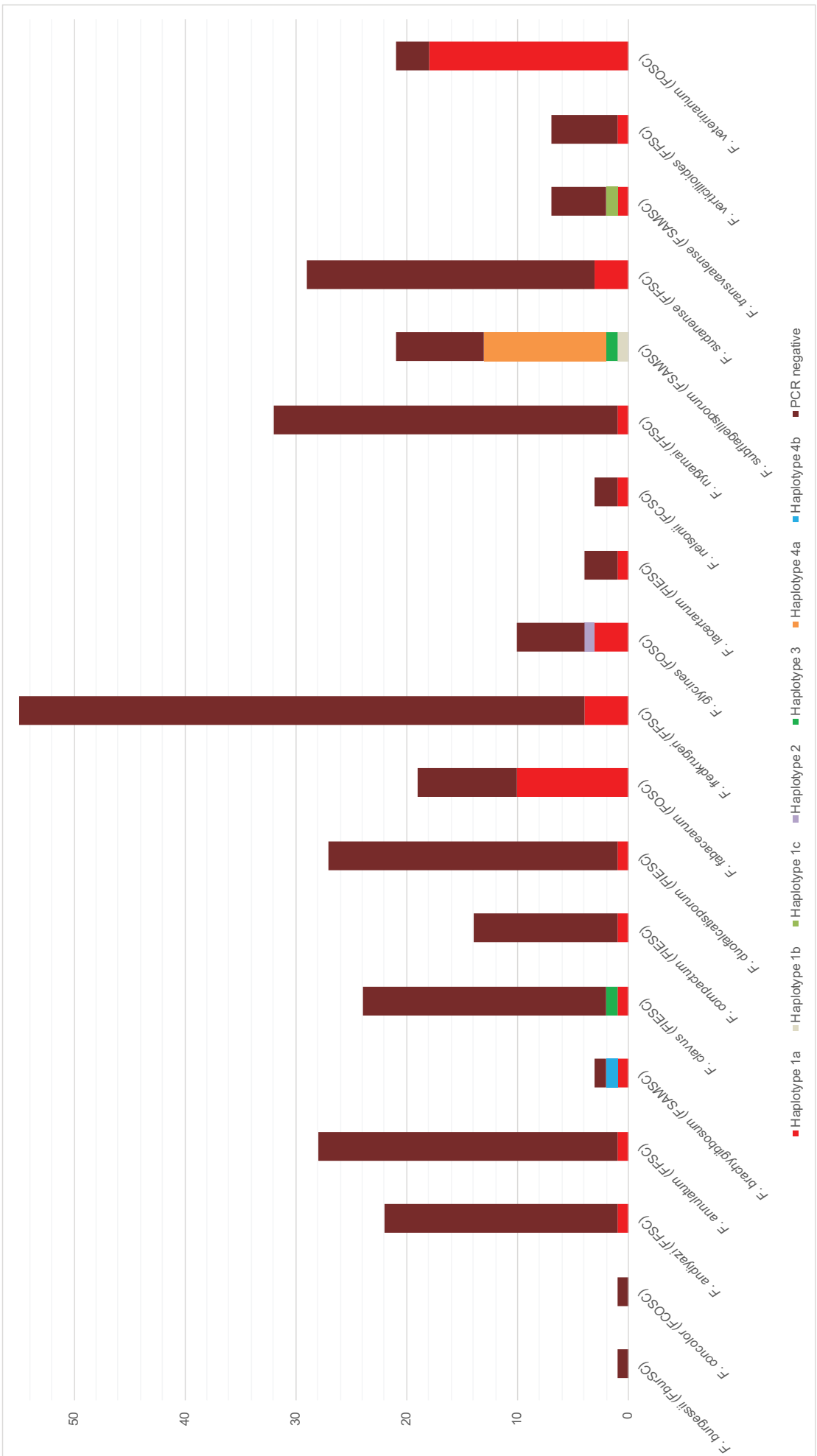

Fig 7. Graph showing the distribution of haplotypes and negative PCR reactions for the striga marker across the tested species. FCSC: *Fusarium chlamydosporum* species complex; FFSC: *Fusarium fujikuroi* species complex; FIESC: *Fusarium incarnatum/equiseti* species complex; FOSC: *Fusarium oxysporum* species complex; FSAMSC: *Fusarium sambucinum* species complex.

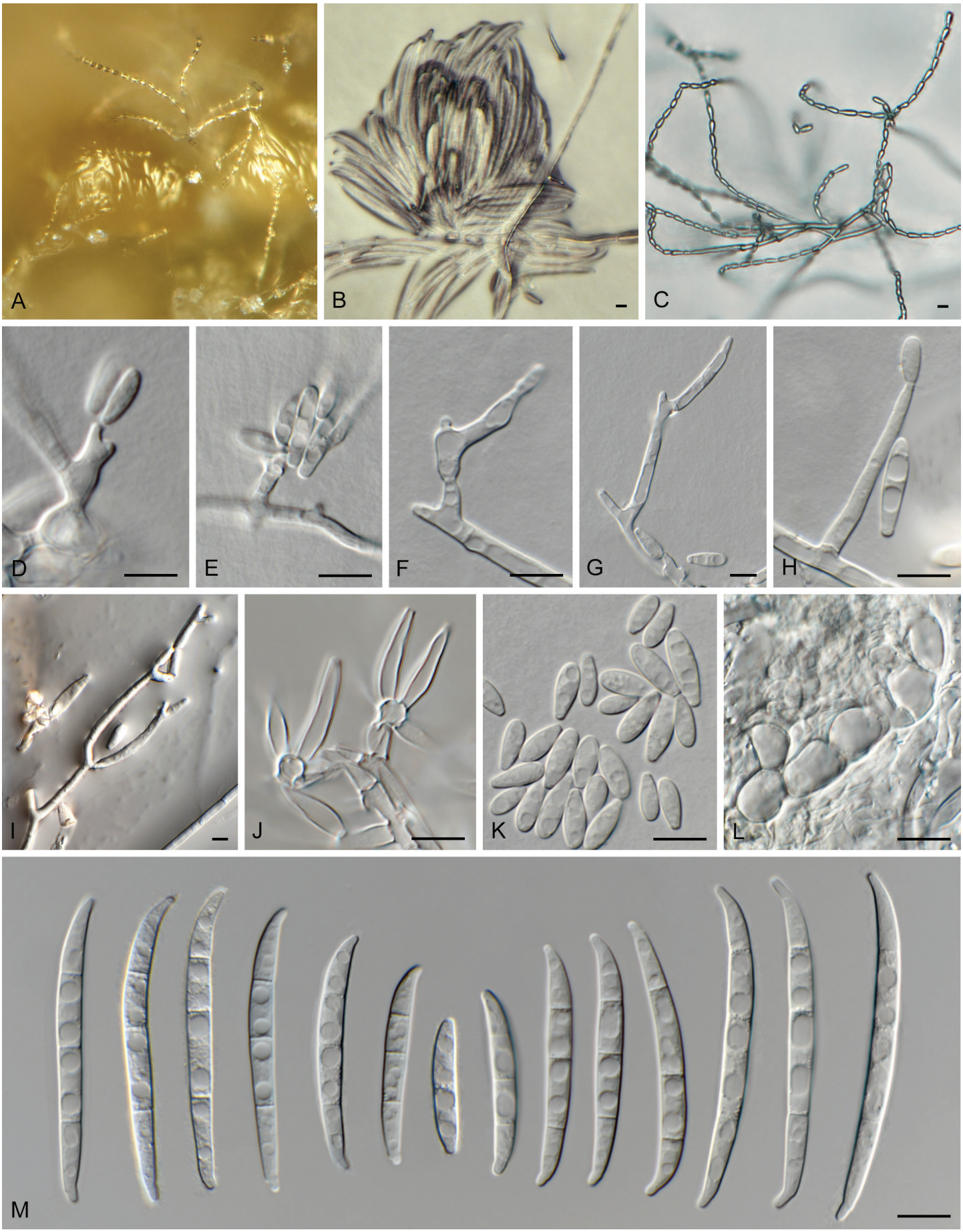

Fig. 8. *Fusarium annulatum* (LLC 782). **A, B.** Sporodochia on SNA. **C.** Chains of microconidia. **D–I.** Mono- and polyphialides giving rise to microconidia. **J.** Sporodochial conidiophores. **K.** Microconidia. **L.** Chlamydospores. **M.** Sporodochial macroconidia. Scale bars = 10 µm.

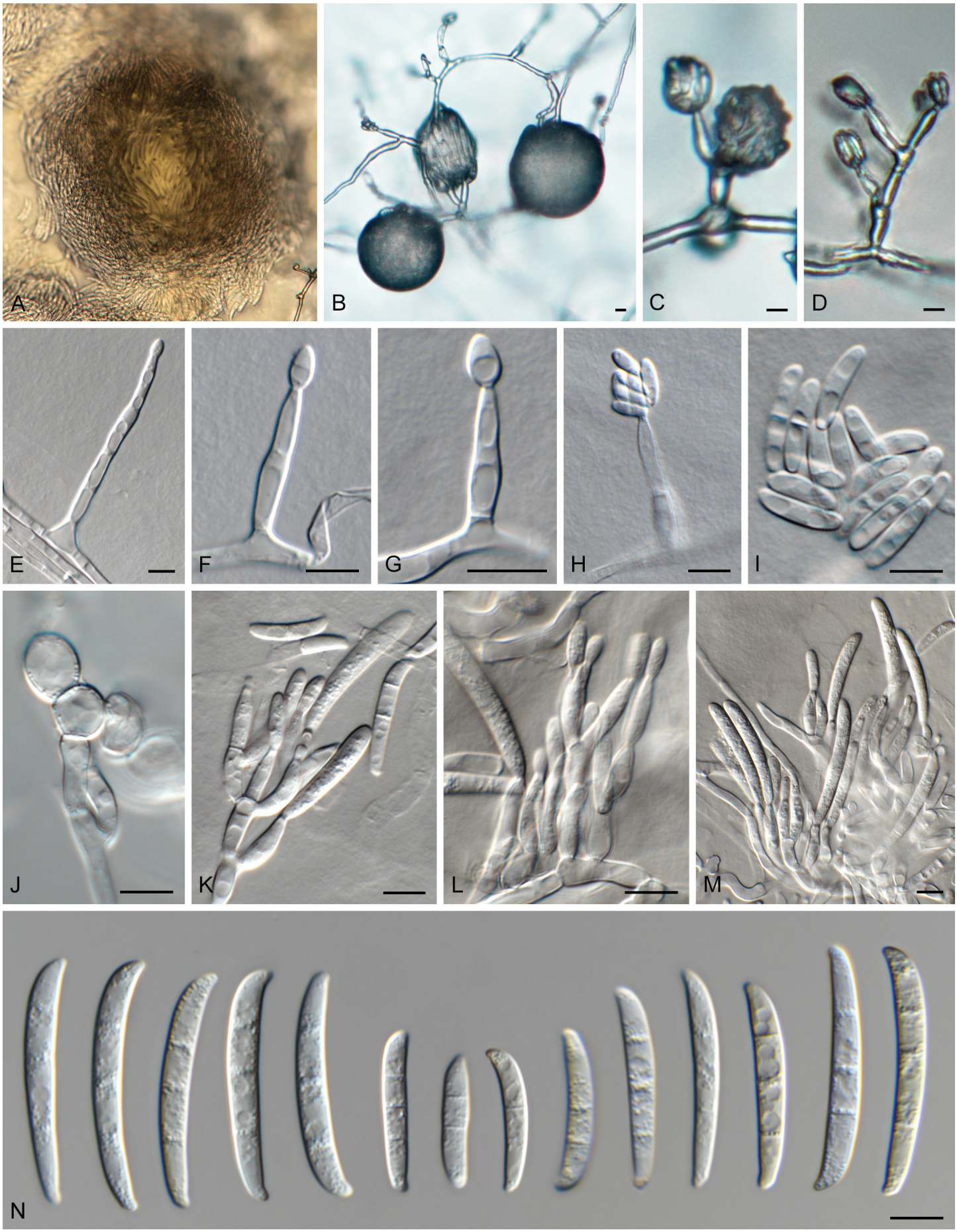

Fig. 9. *Fusarium caapi* (LLC 3528). **A, B.** Sporodochia on SNA. **C–H.** Phialides giving rise to microconidia. **I.** Microconidia. **J.** Chlamydospores. **K–M.** Sporodochial conidiophores. **N.** Sporodochial macroconidia. Scale bars = 10 µm.

Fusarium lactis Pirotta, *Arch. Labor. Bot. Critt. Univ. Pavia* **2 & 3**: 316. 1879. Fig. 10.

Materials examined: Supplementary Table S1.

Notes: The *CaM* sequence of isolate LLC790 is 99.18 % (608/613 nt) identical to the ex-epitype isolate of *F. lactis* (CBS 411.97), the *rpb1* sequence 99.61 % (1 520/1 526 nt), the *rpb2* sequence 99.75 % (797/799 nt), and the *tef1* sequence 97.53 % (633/649 nt).

Fusarium mirum M.M. Costa *et al.*, *Fungal Biol.* **126**: 262. 2022. Fig. 11.

Materials examined: Supplementary Table S1.

Notes: The *F. mirum s.str.* subclade (Fig. 3, part 3) containing the ex-type isolate is highly supported (IQ-TREE bootstrap = 99 % / RAxML bootstrap = 87 % / PP = 0.88) as is the association between LLC917 and *F. mirum s.str.* clades (IQ-TREE bootstrap = 100 % / RAxML bootstrap = 95 % / PP = 1). No *CaM* and *rpb1* sequences were available for comparison to the ex-type isolate of *F. mirum* (CML 3859). The *rpb2* sequence of isolate LLC917 is 99.89 % (897/898 nt) identical to the ex-type isolate of *F. mirum* (CML 3859), and the *tef1* sequence 99.53 % (641/644 nt). As no *CaM* and *rpb1* sequences are available of *F. mirum* and *rpb2* and *tef1* are highly identical to the ex-type isolate of *F. mirum*, we refrain from introducing a new species for this clade at this point.

Fusarium nygamai L.W. Burgess & Trimboli, *Mycologia* **78**: 223. 1986.

Materials examined: Supplementary Table S1.

Notes: The isolates cluster with the ex-type of *F. nygamai* with full support (Fig. 3, part 5). Although there is some genetic variation in the species clade, the internal structure of the species is poorly supported.

Fusarium secorum Secor *et al.*, *Fungal Biol.* **118**: 767. 2014.

Materials examined: Supplementary Table S1.

Notes: The isolate clusters with the ex-type of *F. secorum* with full support (Fig. 3, part 2).

***Fusarium* sp. (LLC1198)**

Materials examined: Supplementary Table S1.

Notes: *Fusarium* sp. LLC1198 (Fig. 3, part 2) is a single isolate basal to the *F. xylarioides* clade. The *F. xylarioides s.str.* subclade containing the ex-type isolate is fully supported (IQ-TREE bootstrap = 100 % / RAxML bootstrap = 100 % / PP = 1) whereas the association between the LLC1198 and *F. xylarioides s.str.* clades was also highly supported (IQ-TREE bootstrap = 100 % / RAxML bootstrap = 94 % / PP = 1). The *CaM* sequence of isolate LLC1198 is 96.98 % (643/663 nt) identical to the ex-type isolate of *F. xylarioides* (CBS 258.52), the *rpb1* sequence (1 525/1 525 nt), the *rpb2* sequence 96.78 % (873/902 nt), and the *tef1* sequence 97.07 % (629/648 nt). Isolate LLC1198 forms part of another study, and will be described elsewhere.

Fusarium sudanense S.A. Ahmed *et al.*, *Antonie van Leeuwenhoek* **110**: 826. 2017.

Materials examined: Supplementary Table S1.

Notes: The isolates cluster as a fully-supported clade sister to the ex-type of *F. sudanense* (Fig. 3, part 5). Although there is some genetic variation in the species clade, the internal structure of the species is poorly supported. The *CaM* sequence of isolate LLC1434 is 99.84 % (612/613 nt) identical to the ex-type isolate of *F. sudanense* (CBS 454.97), the *rpb1* sequence is identical (803/803 nt), the *rpb2* sequence 99.89 % (875/876 nt), and the *tef1* sequence 99.64 % (546/548 nt). Given the high similarity on all four loci with the ex-type isolate of *F. sudanense* we treat this subclade as belonging to that species rather than introducing a new species here.

Fusarium thapsinum Klittich *et al.*, *Mycologia* **89**: 644. 1997.

Materials examined: Supplementary Table S1.

Notes: The isolates cluster interspersed with isolates of *F. thapsinum* (including the ex-type) in a fully-supported clade (Fig. 3, part 3). Although there is quite some genetic variation in the species clade, the internal structure of the species is not to poorly supported.

Fusarium udum E.J. Butler, *Mem. Dept. Agric. India*, Bot. Ser. **2**: 54. 1910.
Synonyms: see www.fusarium.org

Materials examined: Supplementary Table S1.

Notes: The isolates cluster sister to isolates of *F. udum* (including the ex-type) in an almost fully-supported clade (IQ-TREE bootstrap = 100 % / RAxML bootstrap = 99 % / PP = 1; Fig. 3, part 3). Although there is some genetic variation in the species clade, the internal structure of the species is not to poorly supported.

Fusarium verticillioides (Sacc.) Nirenberg, *Mitt. Biol. Bundesanst. Land- Forstw. Berlin-Dahlem* **169**: 26. 1976.
Synonyms: see www.fusarium.org

Materials examined: Supplementary Table S1.

Notes: The isolates cluster sister to isolates of *F. verticillioides* (including the ex-type) in a highly-supported clade (IQ-TREE bootstrap = 98 % / RAxML bootstrap = 86 % / PP = 1; Fig. 3, part 3). Although there is some genetic variation in the species clade, the internal structure of the species is not to poorly supported.

Fusarium incarnatum/equiseti species complex (FIESC)

Fusarium caatingaense A.C.S. Santos *et al.*, Mycologia **111**: 248. 2019.

Materials examined: Supplementary Table S1.

Notes: The isolates cluster interspersed with isolates of *F. caatingaense* (including the ex-type) in an almost fully-supported clade (IQ-TREE bootstrap = 100 % / RAxML bootstrap = 98 % / PP = 1; Fig. 1, part 1). Although there is some genetic variation in

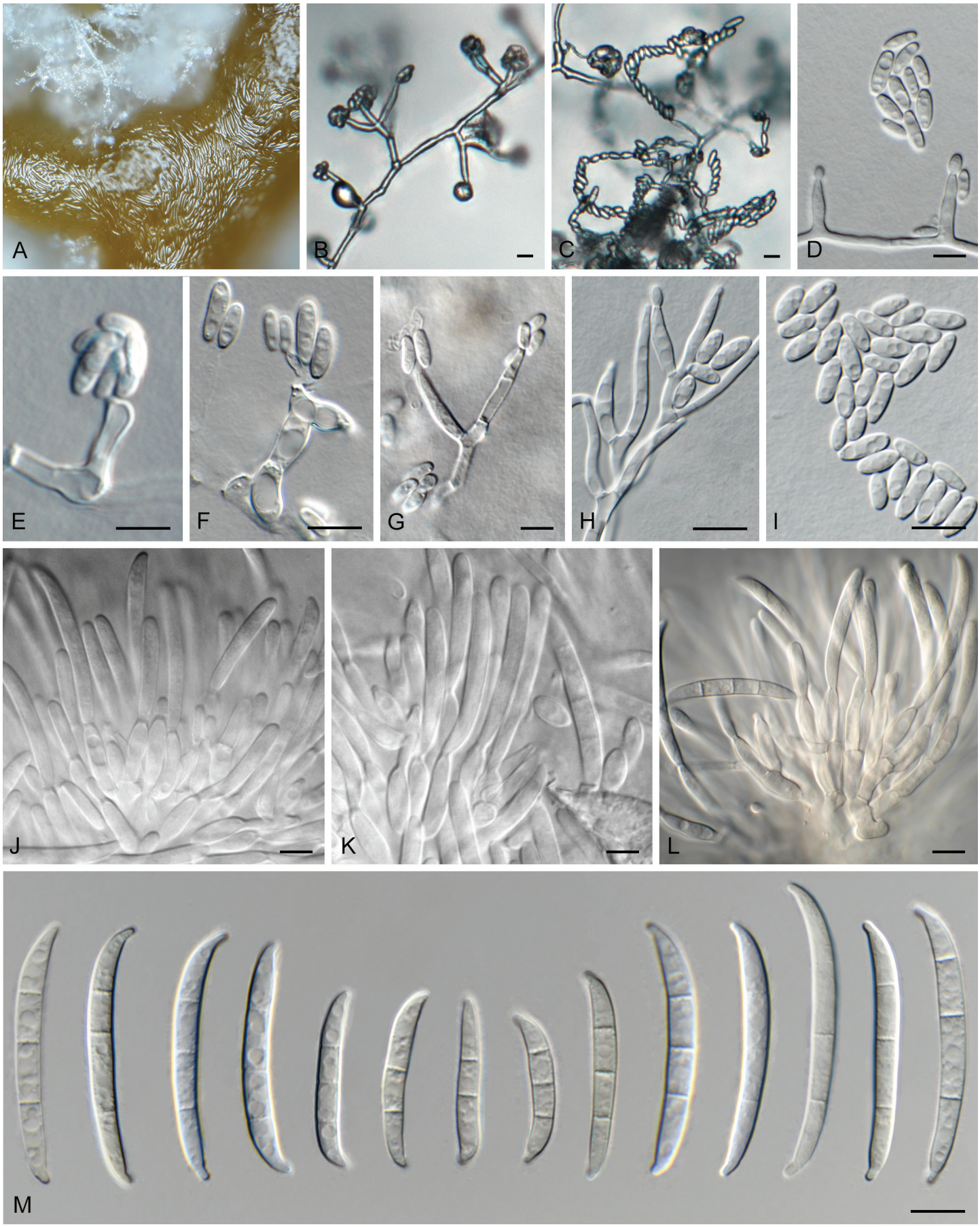

Fig. 10. *Fusarium lactis* (LLC 790). **A.** Sporodochium on SNA. **B–H.** Phialides giving rise to microconidia. **I.** Microconidia. **J–L.** Sporodochial conidiophores. **M.** Sporodochial macroconidia. Scale bars = 10 µm.

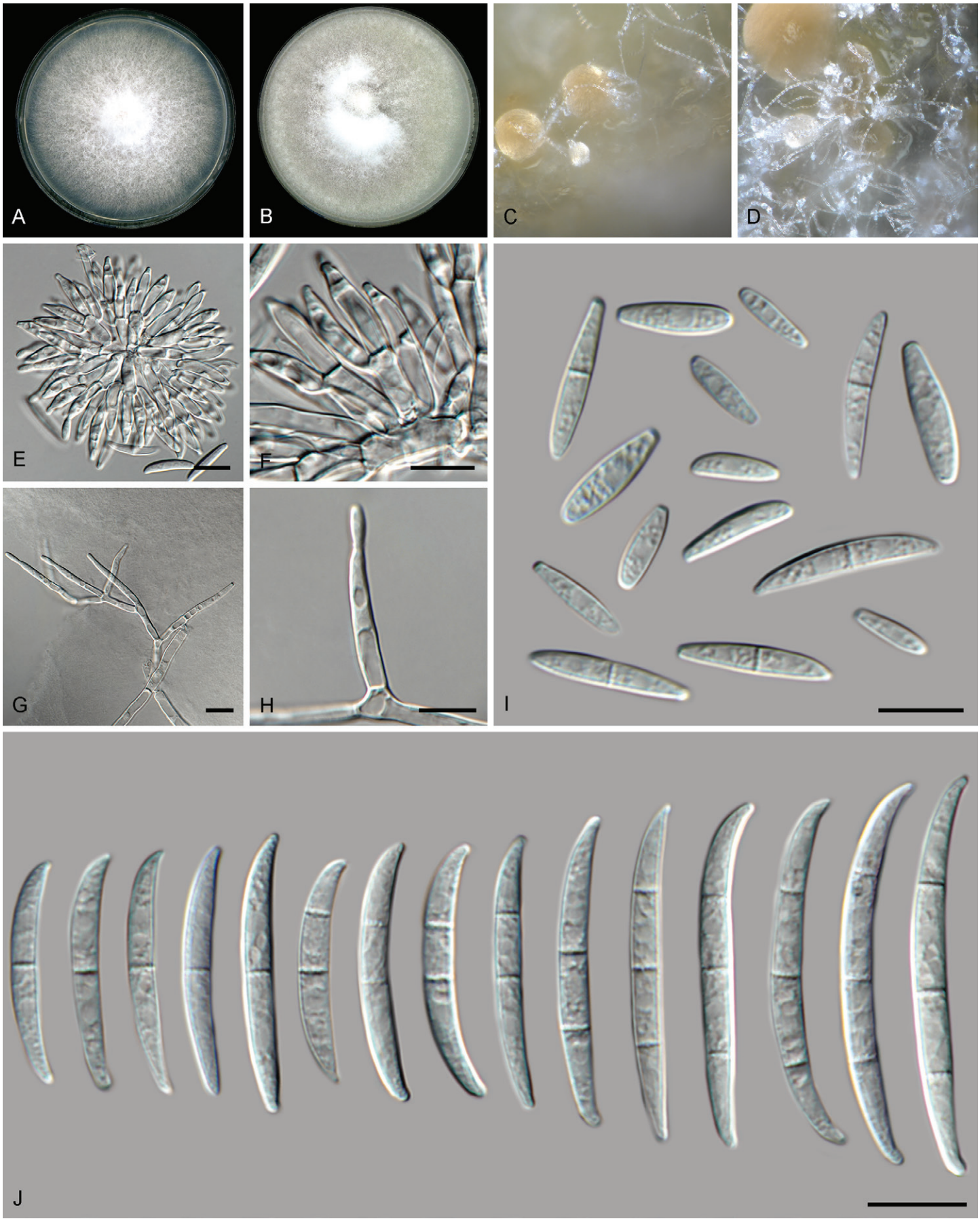

Fig. 11. *Fusarium mirum* (LLC 917). **A.** Colony on PDA. **B.** Colony on OA. **C, D.** Sporodochia. **E, F.** Sporodochial conidiophores. **G, H.** Monophialides on aerial mycelium. **I.** Aerial microconidia. **J.** Sporodochial macroconidia. Scale bars = 10 µm.

the species clade, the internal structure of the species is partly to highly supported but with short branches.

Fusarium clavus J.W. Xia *et al.*, *Persoonia* **43**: 199. 2019.

Materials examined: Supplementary Table S1.

Notes: The isolates cluster interspersed with isolates of *F. clavus* (including the ex-type) in an almost fully-supported clade (IQ-TREE bootstrap = 100 % / RAxML bootstrap = 96 % / PP = 1; Fig. 1, part 2). Although there is some genetic variation in the species clade, the internal structure of the species is partly to highly supported but with short branches.

Fusarium compactum (Wollenw.) Raillo, *Fungi of the Genus Fusarium*: 180. 1950. Fig. 12.
Basionym: *Fusarium scirpi var. compactum* Wollenw., *Fusaria Autographica Delineata* **3**: no. 924. 1930. MB 124046.
Synonyms: see www.fusarium.org

Materials examined: Supplementary Table S1.

Notes: The *F. compactum s.str.* subclade containing the ex-epitype isolate is fully supported whereas the association with isolates LLC1048/LLC1660 and *F. compactum s.str.* clades was not supported (all support values are below the threshold values for display on the tree) (Fig. 1, part 2).

In the phylogenetic tree (Fig. 1, part 2), the *F. compactum* clade consists of two main individually highly supported subclades. The *CaM* sequence of isolate LLC1048 is 98.44 % (567/576 nt) identical to the ex-epitype isolate of *F. compactum* (CBS 186.31). The *rpb1* sequence of isolate LLC1048 is 99.42 % (1 549/1 558 nt) identical to *F. compactum* isolate NRRL 28029 (GenBank HM347150); no *rpb1* sequence is available for the ex-epitype isolate of *F. compactum* (CBS 186.31). The *rpb2* sequence of isolate LLC1048 is 99.89 % (878/879 nt) identical to the ex-epitype isolate of *F. compactum* (CBS 186.31), and the *tef1* sequence 97.02 % (652/672 nt). However, as this subclade is highly similar to *F. compactum* based on three of the four loci used here and only *tef1* is proving to be genetically the most diverse, we choose not to introduce a new species for this subclade pending a further definition of the species boundaries of *F. compactum*.

Fusarium duofalcatisporum J.W. Xia *et al.*, *Persoonia* **43**: 201. 2019.

Materials examined: Supplementary Table S1.

Notes: The isolates cluster interspersed with isolates of *F. duofalcatisporum* (including the ex-type) in a fully-supported clade (Fig. 1, part 2). Although there is some genetic variation in the species clade, the internal structure of the species is partly to highly supported but with short branches.

Fusarium extenuatum L. Lombard, *sp. nov*. — MycoBank MB 846717. Fig. 13.

Etymology: Name refers to the conidiophores that are reduced to lateral phialides on the aerial mycelium.

Typus: **Ethiopia**, Tigray Region, Central (Meakelewi) Zone, Tanqua Abergele District, Yechela locality (Kebele), from soil collected in a sorghum field, 2017, *D.W. Etolo & L. Lombard* (**holotype** EMCC-F333, preserved as metabolic inactive culture, culture ex-type LLC1501 = EMCC-F333).

Conidiophores reduced to solitary conidiogenous cells borne laterally on hyphae; *aerial conidiogenous cells* monophialides, subulate to subcylindrical, smooth- and thin-walled, 14–22 × 4 µm, periclinal thickening and collarettes often inconspicuous. *Aerial macroconidia* similar to sporodochial conidia. *Sporodochial conidiophores* 22–38 µm tall, irregularly branched, bearing terminal solitary or whorls of 2–3 phialides. *Sporodochial conidiogenous cells* monophialidic, doliiform, subulate to subcylindrical, smooth- and thin-walled, (10–)11–13(–15) × (3–)4–5 µm. *Sporodochial conidia* straight to moderately curved and slender, tapering towards the basal part, apical cell elongated (papillate) to whip-like; basal cell well-developed, foot-shaped, mostly papillate, (3–)5(–6)-septate, hyaline, thin- and smooth-walled: 3-septate conidia 32–46(–61) × (3–)4–5 µm (av. 38 × 5 µm) ; 4-septate conidia (34–)36–40(–42) × 4–5 µm (av. 38 × 5 µm); 5-septate conidia (49–)47–69(–73)× (3–)4–5 µm (av. 63 × 4 µm); 6-septate conidia (75–)77–87(–90) × (4–)5–6 µm (av. 82 × 5 µm; *n* = 7). *Chlamydospores* not observed.

Culture characteristics: Colonies on PDA reaching 85–90 mm diam at 25 °C after 7 d. Surface white with luteus to amber flames, raised, woolly to cottony with abundant aerial mycelium, margin regular and filiform. Reverse pale luteus. On OA, white to amber, raised, woolly to cottony with abundant aerial mycelium, margin regular and filiform. Reverse pale luteus.

Additional materials examined: Supplementary Table S1.

Notes: *Fusarium extenuatum* represents a unique fully-supported clade in the Equiseti Clade (Xia *et al.* 2019) in the FIESC. Although morphologically similar to *F. longifundum*, this species did not produce any chlamydospores in culture. In addition, these two species are not closely related in the phylogenetic tree (Fig. 1, part 1 *vs* part 2).

In the phylogenetic tree (Fig. 1, part 2), the *F. clavus s.l.* clade consists of three main highly supported subclades. The *F. clavus* clade at its most basal position is highly supported in two of the three analyses (IQ-TREE bootstrap = 99 % / RAxML bootstrap < 75 % / PP = 1); the third subclade contains the species' ex-type isolate and is highly supported (IQ-TREE bootstrap = 100 % / RAxML bootstrap = 96 % / PP = 1). The first subclade is described here as *F. extenuatum sp. nov.*; see *F. tangerinum* below for a discussion on the second subclade. The *CaM* sequence of isolate LLC1501 from this subclade is 98.69 % similar (527/534 nt) to that of *F. ipomoeae* isolate LC12163 and 98.0 % similar (539/550 nt) to the ex-type isolate of *F. clavus* (CBS 126202). The *rpb1* sequence of isolate LLC1501 is most identical to *F. equiseti* isolate NL19-97009 (835/841 nt = 99.29 %). No *rpb1* sequence is available for the ex-type isolate of *F. clavus*, but a comparison to the *rpb1* sequence of *F. clavus* isolate JW 288002 reveals a similarity of 98.26 % (789/803 nt). The *rpb2* sequence of isolate LLC1501 is 97.74 % similar (820/839 nt) to that of the ex-type isolate of *F. clavus* (CBS 126202). The *tef1* sequence of isolate LLC1501 is 94.81 % identical (566/597 nt) to that of the ex-type isolate of *F. clavus* (CBS 126202).

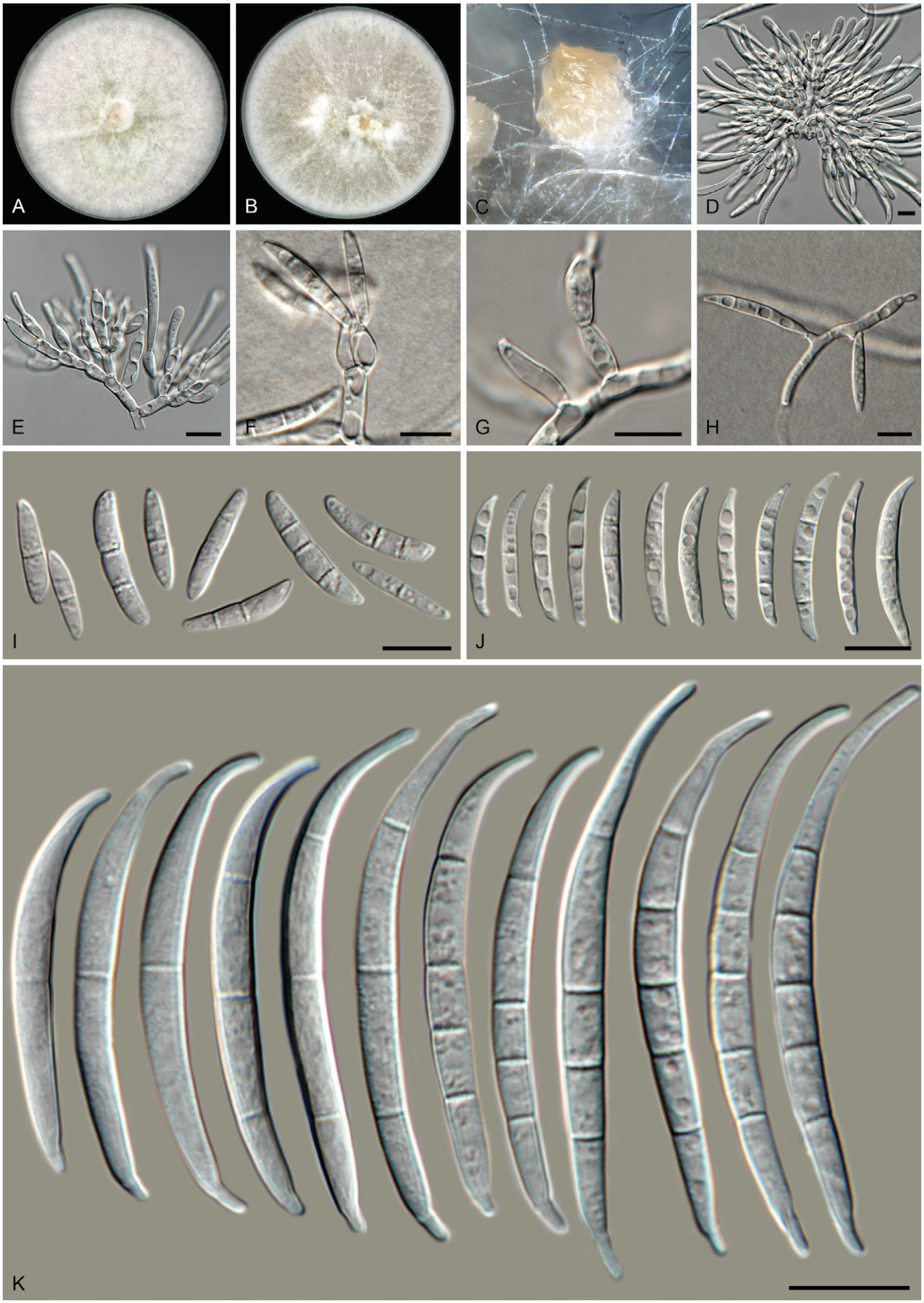

Fig. 12. *Fusarium compactum* (LLC 1660). **A.** Colony on PDA. **B.** Colony on OA. **C.** Sporodochium on carnation leaves. **D, E.** Sporodochia and sporodochial conidiophores. **F–H.** Phialides on aerial mycelium. **I, J.** Aerial macroconidia. **K.** Sporodochial macroconidia. Scale bars = 10 µm.

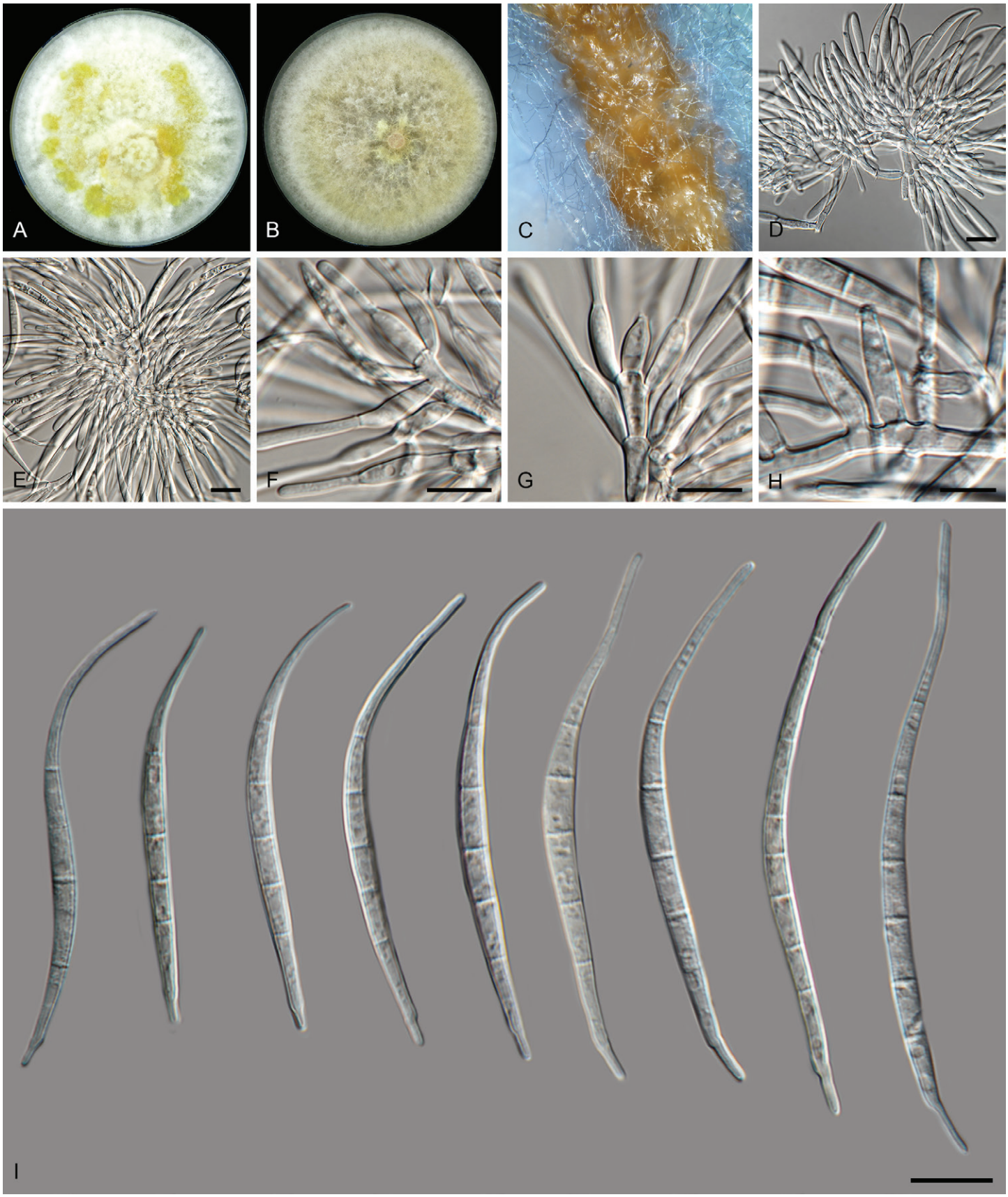

Fig. 13. *Fusarium extenuatum* **(**LLC 1501). **A.** Colony on PDA. **B.** Colony on OA. **C.** Sporodochia on carnation leaves. **D, E.** Sporodochia. **F–H.** Sporodochial conidiophores. **I.** Sporodochial macroconidia. Scale bars = 10 µm.

Fusarium incarnatum (Desm.) Sacc., *Syll. Fung.* (Abellini) **4**: 712. 1886. Fig. 14.

Materials examined: Supplementary Table S1.

Notes: In the phylogenetic tree (Fig. 1, part 1), the *F. incarnatum* clade consists of two subclades not supported in any of phylogenetic analyses. The *F. incarnatum* clade itself is moderately supported in the IQ-TREE analysis (88 %), not supported in the

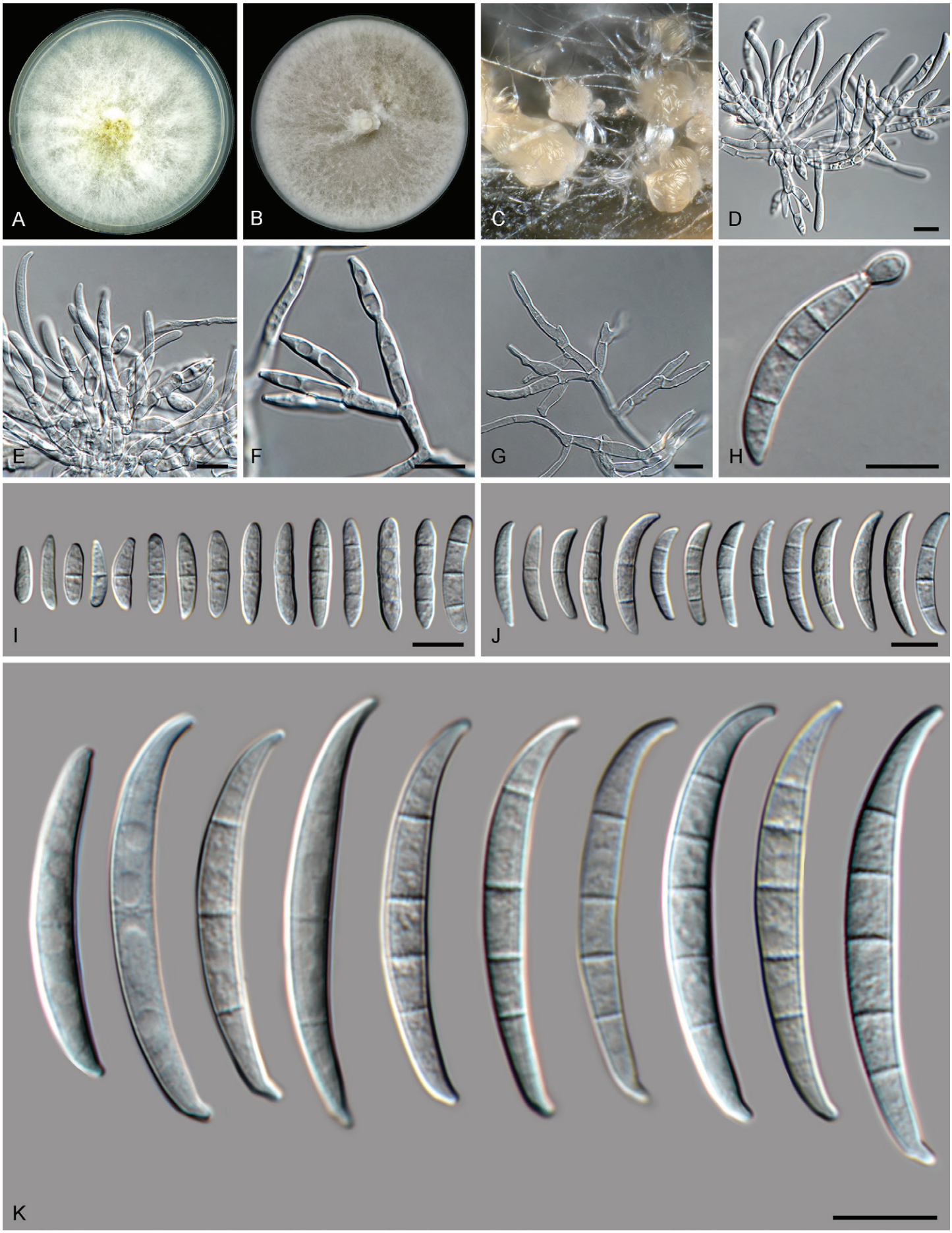

Fig. 14. *Fusarium incarnatum* (LLC 1220). **A.** Colony on PDA. **B.** Colony on OA. **C.** Sporodochia on carnation leaves. **D, E.** Sporodochia and sporodochial conidiophores. **F, G.** Conidiophores with mono- and polyphialides on aerial mycelium. **H.** Microcyclic conidiogenesis. **I.** Aerial microconidia. **J.** Aerial macroconidia. **K.** Sporodochial macroconidia. Scale bars = 10 µm.

RAxML analysis (< 75 %) and highly supported in the Bayesian analysis (PP = 0.98). The *CaM* sequence of isolate LLC1220 from the second subclade is identical (549/549 nt) to that of the ex-epitype isolate of *F. incarnatum* (CBS 132.73) in the first subclade whereas the *rpb1* sequence is more identical to *F. guilinense* isolate FRC R-8480 (793/798 nt = 99.37 %). No *rpb1* sequence is available for the ex-epitype of *F. incarnatum* but a comparison to the *rpb1* sequence of *F. incarnatum* isolate NRRL 32866 reveals a similarity of 98.75 % (788/798 nt). The *rpb2* sequence of isolate LLC1220 differs 7 nt from several species such as *F. caatingaense*, *F. nanum* and *F. hainanense* while it is 98.81 % identical (829/839 nt) to that of the ex-epitype isolate of *F. incarnatum* (CBS 132.73). The *tef1* sequence of isolate LLC1220 is 99.83 % identical (599/600 nt) to that of the ex-epitype isolate of *F. incarnatum* (CBS 132.73). Given that both intron-rich genes *CaM* and *tef1* are identical to almost identical to *F. incarnatum,* and *rpb1* and *rpb2* only have up to 10 nt differences, we refrain for now from introducing a new species for the second clade and treat it as *F. incarnatum*.

Fusarium lacertarum Subrahm. [as '*laceratum*'], *Mykosen* **26**: 478. 1983.

Materials examined: Supplementary Table S1.

Notes: The *F. lacertarum s.str.* subclade containing the ex-type isolate is highly supported (IQ-TREE bootstrap = 100 % / RAxML bootstrap = 99 % / PP = 1) and the association between the clade containing isolate LLC2984 and the *F. lacertarum s.str.* clade is also highly supported (IQ-TREE bootstrap = 100 % / RAxML bootstrap = 97 % / PP = 1).

In the phylogenetic tree (Fig. 1, part 2), the *F. lacertarum* clade consists of two main highly supported subclades. The *CaM* sequence of isolate LLC2984 is 99.09 % (546/551 nt) identical to the ex-type isolate of *F. lacertarum* (CBS 130185). No *rpb1* sequences of isolates belonging to LLC2984 are available for comparison to the ex-type isolate of *F. lacertarum* (CBS 130185). The *rpb2* sequence of isolate LLC2984 is 98.98 % (870/879 nt) identical to the ex-type isolate of *F. lacertarum* (CBS 130185). The *tef1* sequence of isolate LLC2984 is 98.80 % (661/669 nt, including a single indel of 3 nt) identical to the ex-type isolate of *F. lacertarum* (CBS 130185). However, as this subclade is highly similar to *F. lacertarum* based on three available loci used here, we choose not to introduce a new species for this subclade pending a further definition of the species boundaries of *F. lacertarum*.

Fusarium nanum M.M. Wang *et al.*, *Persoonia* **43**: 85. 2019.

Materials examined: Supplementary Table S1.

Notes: The isolates cluster interspersed with isolates of *F. nanum* (including the ex-type) in a partly-supported clade (IQ-TREE bootstrap = 98 % / RAxML bootstrap = 90 % / PP = 0.98; Fig. 1, part 1). Although there is some genetic variation in the species clade, the internal structure of the species is partly supported but with short branches.

Fusarium serpentinum J.W. Xia *et al.*, *Persoonia* **43**: 217. 2019.

Materials examined: Supplementary Table S1.

Note: The isolate clusters with the ex-type isolate of *F. serpentinum* in a fully-supported clade (Fig. 1, part 1).

Fusarium tangerinum Crous, Sand.-Den. & M.M. Costa, *sp. nov*. MycoBank MB 846718. Fig. 15, 16.

Etymology: Name refers to its abundant, orange sporodochia.

Typus: **Ethiopia**, Amhara Region, Oromia Zone, Artuma Fursi District, Hula Tukuye locality (Kebele), from *Sorghum* cv. Teshale rhizosphere soil field, 2019, *D.W. Etolo & L. Lombard* (**holotype** EMCC-F377, preserved as metabolically inactive culture, culture ex-type LLC3501 = EMCC-F377).

Aerial conidiophores sparingly branched, 15–40 µm tall, bearing terminal, rarely lateral monophialides (polyphialides rarely observed), mostly reduced to conidiogenous cells on hyphae; aerial conidiogenous cells monophialidic, subulate to subcylindrical, thin-walled, 10–25 × 2.5–3 µm, with flared collarette and minute periclinal thickening. *Aerial conidia* aggregating in false heads, fusoid-ellipsoid, aseptate, apex subobtuse, base truncate, (6–)8–9(–11) × (2–)2.5(–3) µm. *Sporodochia* orange, abundant on CLA. *Sporodochial conidiophores* densely aggregated, branched, consisting of a stipe bearing whorls or 2–4 monophialides; *sporodochial conidiogenous cells* monophialidic, subulate to subcylindrical, 8–20 × 3.5–5 µm, smooth- and thin-walled with periclinal thickening and minute collarette. *Sporodochial conidia* falcate, curved dorsiventrally, tapering from middle towards both ends; apical cell elongated, hooked, whip-like with parallel sides and subobtuse apex; basal cell foot-shaped, notch well developed, (3–)5-septate, hyaline, smooth-walled, guttulate; 3-septate conidia (23–)30–40(–44) × (3.5–)4(–5) µm, 5-septate conidia (40–)45–50(–55) × (4–)4.5(–5) µm. *Chlamydospores* on SNA after 1 wk, solitary or in groups of 2–3, terminal or intercalary, subglobose, 8–12 µm diam.

Culture characteristics: Colonies erumpent, spreading, covering dish after 7 d at 25 °C. On PDA surface and reverse saffron; on OA surface saffron, reverse saffron to dark vinaceous.

Additional material examined: Supplementary Table S1.

Notes: *Fusarium tangerinum* is proposed here for the second fully supported clade in the *F. clavus s.l.* clade; also see *F. extenuatum sp. nov*. above.

In the phylogenetic tree (Fig. 1, part 2), the *F. clavus* clade consists of three main highly supported subclades. The *CaM* sequence of isolate LLC3018 from the second subclade is 98.06 % (555/566 nt) and 99.27 % (546/550 nt) identical to the ex-type isolates of *F. extenuatum* (LLC1501) and *F. clavus* (CBS 126202), respectively. No *rpb1* sequence is available for isolate LLC3018 and therefore the sequence of isolate LLC3501 was used for comparison. The *rpb1* sequence of isolate LLC3501 is 96.42 % (727/754 nt) identical to the ex-type isolate of *F. extenuatum* (LLC1501). No *rpb1* sequence is available for the ex-type isolate of *F. clavus* (CBS 126202), but a comparison to the *rpb1* sequence of *F. clavus* isolate JW 288002 reveals a similarity of 96.55 % (728/754 nt). The *rpb2* sequence of isolate LLC3018 is 97.67 % (713/730 nt) and 96.99 % (708/730 nt) identical to the ex-type isolates of *F. extenuatum* (LLC1501) and *F. clavus* (CBS 126202), respectively. The *tef1* sequence of isolate LLC3018 is 94.09 % (637/677 nt) and 96.64 % (575/595 nt) identical to the ex-type isolates of *F. extenuatum* (LLC1501) and *F. clavus* (CBS 126202), respectively.

Fig. 15. *Fusarium tangerinum* (LLC 3501). **A–C.** Sporodochia on SNA. **D–F.** Phialides giving rise to microconidia. **G.** Microconidia. **H.** Chlamydospores. **I–L.** Sporodochial conidiophores. **M.** Sporodochial macroconidia. Scale bars = 10 µm.

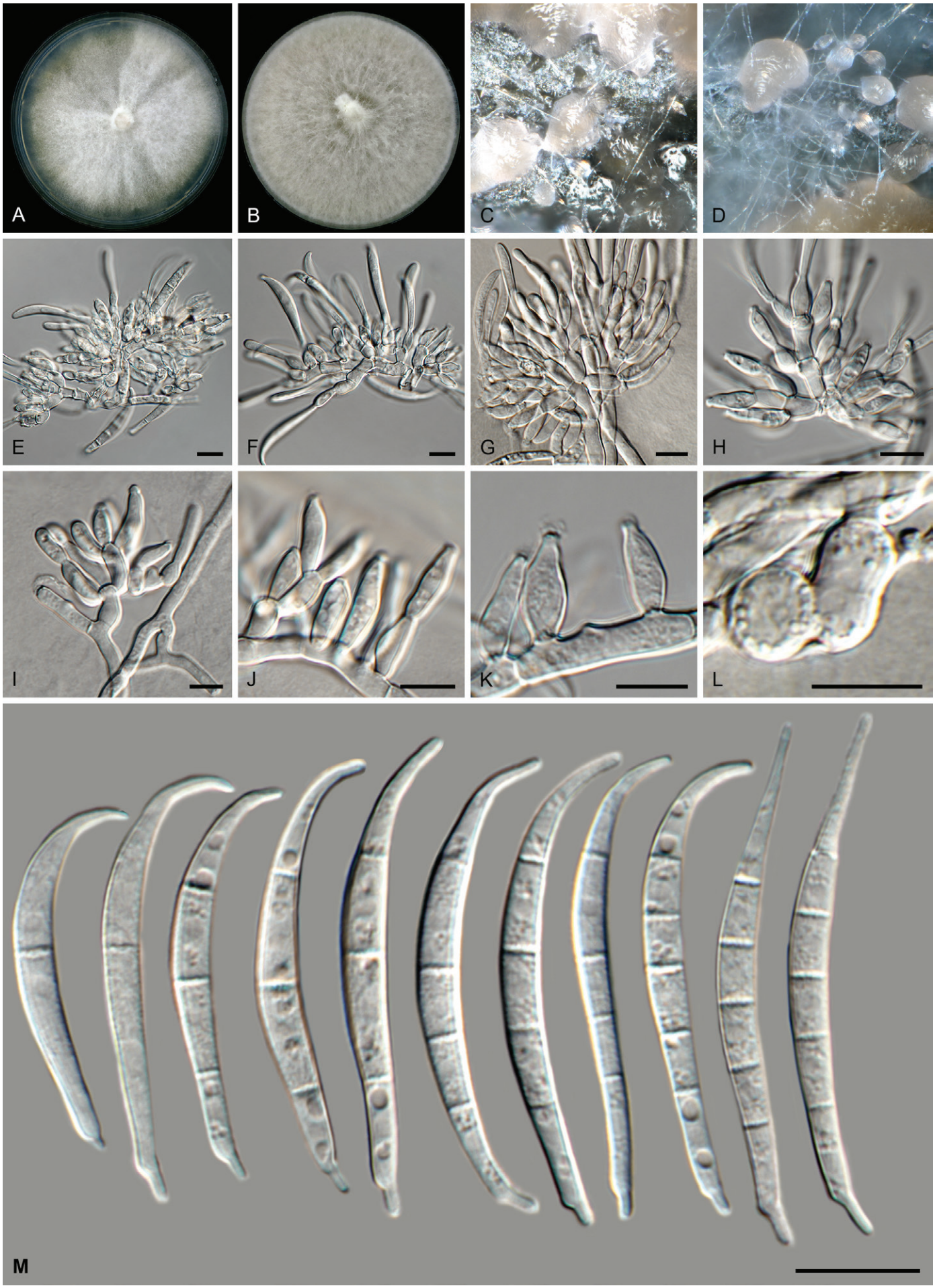

Fig. 16. *Fusarium tangerinum* (LLC 3018). **A.** Colony on PDA. **B.** Colony on OA. **C, D.** Sporodochia. **E–H.** Sporodochial conidiophores. **I–K.** Monophialides on aerial mycelium. **L.** Chlamydospores. **M.** Sporodochial macroconidia. Scale bars = 10 µm.

Fusarium oxysporum species complex (FOSC)

Fusarium curvatum L. Lombard & Crous, *Persoonia* **41**: 21. 2018.

Materials examined: Supplementary Table S1.

Notes: The *F. curvatum s.str.* subclade containing the ex-type isolate is poorly supported (IQ-TREE bootstrap = 89 % / RAxML bootstrap = < 75 % / PP = <0.74; Fig. 4, part 1) and the node including LLC2077 only receives support from the Bayesian analysis (PP = 0.95). The *CaM* sequence of isolate LLC2077 is identical (559/559 nt) to the ex-type isolate of *F. curvatum* (CBS 238.94), the *rpb1* sequence 99.88 % (1 665/1 667 nt), the *rpb2* sequence is identical (877/877 nt), and the *tef1* sequence 99.31 % (577/581 nt). Due to the absent to minor differences between LLC2077 and the ex-type isolate of *F. curvatum* (CBS 238.94), we treat this isolate as *F. curvatum*.

Fusarium fabacearum L. Lombard *et al.*, *Persoonia* **43**: 24. 2019. Fig. 17.
New synonym: *Fusarium tardicrescens* Maryani *et al.*, *Persoonia* **43**: 69. 2019.

Materials examined: Supplementary Table S1.

Notes: The isolates are interspersed with isolates previously treated as *F. fabacearum* and *F. tardicrescens* (including the ex-types of both species) in an unresolved clade (Fig. 4, part 2). As no *CaM* sequence is available for the ex-type isolate of *F. tardicrescens* (CBS 102024), the *CaM* sequence of isolate LLC2199 was compared to that of *F. tardicrescens* isolate JW 6021 and a 99.66 % similarity (590/592 nt) was found. The *CaM* sequence of isolate LLC2199 is 99.32 % (588/592 nt) identical to the ex-type isolate of *F. fabacearum* (CBS 144743). The *rpb1* sequence of isolate LLC2199 is 99.66 % (879/882 nt) and 99.87 % (791/792 nt) identical to the ex-type isolates of *F. fabacearum* (CBS 144743) and *F. tardicrescens* (CBS 102024), respectively. The *rpb2* sequence of isolate LLC2199 is identical (877/877 and 835/835 nt) to the ex-type isolates of *F. fabacearum* (CBS 144743) and *F. tardicrescens* (CBS 102024), respectively. The *tef1* sequence of isolate LLC2199 is 99.67 % (613/615 nt) and 100 % (574/574 nt) identical to the ex-type isolates of *F. fabacearum* (CBS 144743) and *F. tardicrescens* (CBS 102024), respectively. In the present study, we treat all newly sequenced isolates under the earlier validly described name *F. fabacearum* (Lombard *et al.* 2019; published online 18 Dec. 2018) rather than the later possible synonym *F. tardicrescens* (Maryani *et al.* 2019a; invalidly published online 5 Jul. 2018, validated by Maryani *et al.* 2019b on 14 Mar. 2019).

Fusarium glycines L. Lombard *et al.*, *Persoonia* **43**: 25. 2018.

Materials examined: Supplementary Table S1.

Notes: The isolates cluster interspersed with isolates of *F. glycines* (including the ex-type) in a partly-supported clade (IQ-TREE bootstrap = 99 % / RAxML bootstrap = < 75 % / PP = 1; Fig. 4, part 2). Although there is some genetic variation in the species clade, the internal structure of the species is only partly supported.

Fusarium gossypinum L. Lombard & Crous, *Persoonia* **43**: 26. 2018.

Materials examined: Supplementary Table S1.

Notes: The isolates cluster with isolates of *F. gossypinum* (including the ex-type) in an unresolved clade (Fig. 4, part 2). Although there is some genetic variation, there is no internal structure.

Fusarium libertatis L. Lombard & Crous, *Persoonia* **41**: 29. 2018.

Materials examined: Supplementary Table S1.

Notes: The *F. libertatis s.str.* subclade containing the ex-type isolate is well-supported (IQ-TREE bootstrap = 100 % / RAxML bootstrap = 78 % / PP = 1) and the node including LLC1736 also receives high support (IQ-TREE bootstrap = 99 % / RAxML bootstrap = 84 % / PP = 1). The *CaM* sequence of isolate LLC1736 is identical (602/602 nt) to the ex-type isolate of *F. libertatis* (CBS 144749). No *rpb1* sequence are available for isolates of *F. libertatis* and therefore comparisons were not possible. The *rpb2* sequence of isolate LLC1736 is 99.89 % (876/877 nt) identical to the ex-type isolate of *F. libertatis* (CBS 144749), and the *tef1* sequence 99.31 % (577/581 nt). Due to the absent to minor differences between LLC2077 and the ex-type isolate of *F. libertatis* (CBS 144749), we treat this isolate as *F. libertatis*.

Fusarium odoratissimum Maryani *et al.*, *Stud. Mycol.* **92**: 159. 2018. Fig. 18.

Materials examined: Supplementary Table S1.

Notes: Isolate LLC706 clustered in a highly-supported clade, closely related to *F. odoratissimum* and *F. phialophorum*. In the phylogenetic tree (Fig. 4, part 1), the clade containing LLC706 is almost fully supported (IQ-TREE bootstrap = 99 % / RAxML bootstrap = 99 % / PP = 1). As no *CaM* sequences are available for the ex-type isolate of *F. odoratissimum* (InaCC F822) and for none of the isolates of *F. phialophorum*, the *CaM* sequence of isolate LLC706 was only compared to *F. odoratissimum* (isolates JW 54001 and CBS 102030), and a 100 % similarity (574/574 and 570/570 nt), was found. The *rpb1* sequence of isolate LLC706 is 98.38 % (1 338/1 360 nt) and 99.10 % (1 431/1 444 nt) identical to the ex-type isolates of *F. odoratissimum* (InaCC F822) and *F. phialophorum* (InaCC F971), respectively. The *rpb2* sequence of isolate LLC706 is 99.77 % (858/860 nt) and 99.77 % (858/860 nt) identical to the ex-type isolates of *F. odoratissimum* (InaCC F822) and *F. phialophorum* (InaCC F971), respectively. The *tef1* sequence of isolate LLC706 is 99.48 % (569/572 nt) and 99.65 % (570/572 nt) identical to the ex-type isolates of *F. odoratissimum* (InaCC F822) and *F. phialophorum* (InaCC F971), respectively. However, as this subclade is highly similar to both *F. odoratissimum* and *F. phialophorum* based on the loci used here and only *rpb1* is proving to be genetically the most diverse, we choose not to introduce a new species for this subclade pending a further definition of the species boundaries of *F. odoratissimum* and *F. phialophorum*.

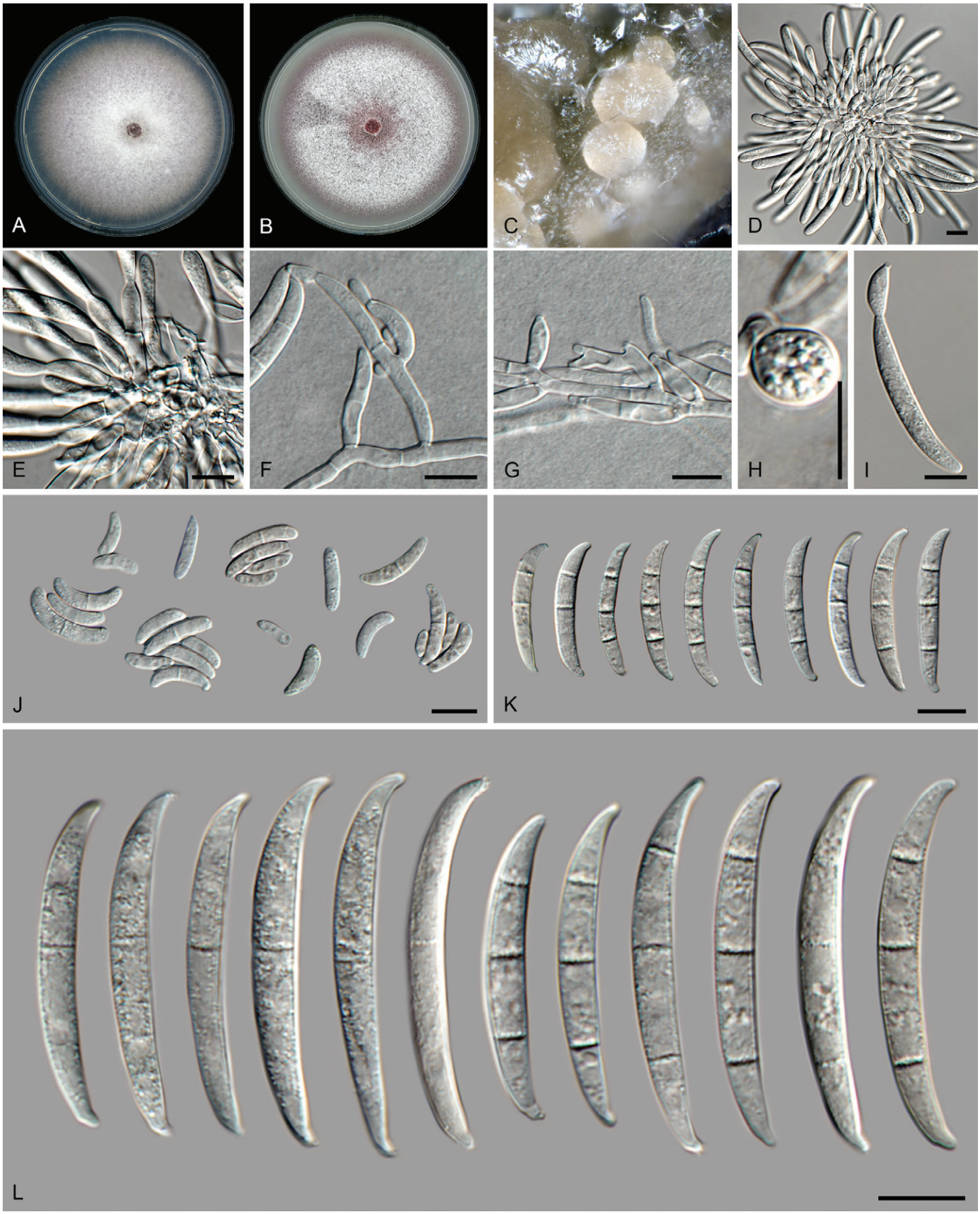

Fig. 17. *Fusarium fabacearum* (LLC 2199). **A.** Colony on PDA. **B.** Colony on OA. **C.** Sporodochia on carnation leaves. **D, E.** Sporodochia and sporodochial conidiophores. **F, G.** Conidiophores with mono- and polyphialides on aerial mycelium. **H.** Chlamydospore. **I.** Microcyclic conidiogenesis. **J.** Aerial microconidia. **K.** Aerial macroconidia. **L.** Sporodochial macroconidia. Scale bars = 10 µm.

Fig. 18. *Fusarium odoratissimum* (LLC 706). **A.** Colony on PDA. **B.** Colony on OA. **C.** Sporodochia on carnation leaves. **D, E.** Sporodochia and sporodochial conidiophores. **F, G.** Lateral conidiogenous cells on aerial mycelium. **H.** Chlamydospore. **I.** Aerial microconidia. **J.** Sporodochial macroconidia. Scale bars = 10 µm.

***Fusarium* sp. 1**

Materials examined: Supplementary Table S1.

Notes: The isolate clusters with two isolates of *Fusarium* sp. 1 *sensu* Crous *et al*. (2021a) in a moderately to highly supported clade (IQ-TREE bootstrap = 99 % / RAxML bootstrap = 76 % / PP = 1; Fig. 4, part 2). The species was treated by Crous *et al*. (2021a), but not formally described as none of the loci used could individually discriminate it as unique. The long branch for this isolate is due to the missing *rpb2* sequence.

Fusarium veterinarium L. Lombard & Crous, *Persoonia* **41**: 35. 2018. Figs 19.

Materials examined: Supplementary Table S1.

Notes: In the phylogenetic tree (Fig. 4, part 1), the *F. veterinarium s.l.* clade is not supported above the display threshold values (IQ-TREE bootstrap = >84 % / RAxML bootstrap = >74 % / PP = >0.74) and none of the internal "subclades" receive any significant support. No *CaM* and *rpb2* sequences are available for LLC3779, therefore comparisons were made using the sequences of LLC3901. The *CaM* sequence of isolate LLC3901 is 99.83 % (601/602 nt) identical to the ex-type isolate of *F. veterinarium* (CBS 109898). No *rpb1* sequences of *F. veterinarium* isolates were available for comparison. The *rpb2* sequence of isolate LLC3901 is 99.89 % (876/877 nt) identical to the ex-type isolate of *F. veterinarium* (CBS 109898), and the *tef1* sequence 99.51 % (613/616 nt). The *CaM* sequence of isolate LLC3929 is identical (580/580 nt) to the ex-type isolate of *F. veterinarium* (CBS 109898). No *rpb1* sequences of *F. veterinarium* isolates were available for comparison. The *rpb2* sequence of isolate LLC3929 is identical (877/877 nt) to the ex-type isolate of *F. veterinarium* (CBS 109898). The *tef1* sequence of isolate LLC3929 is identical (423/423 nt) to the ex-type isolate of *F. veterinarium* (CBS 109898). The observed tree topology seems to be an artifact of the missing *F. veterinarium rpb1* sequences and the isolates are therefore treated as belonging to *F. veterinarium*.

Fusarium sambucinum species complex (FSAMSC)

Fusarium brachygibbosum Padwick, *Mycol. Pap.* **12**: 11. 1945. Fig. 20.

Materials examined: Supplementary Table S1.

Notes: In the phylogenetic tree (Fig. 2), the *F. brachygibbosum s.l.* clade is fully supported and the two internal subclades were fully supported and highly supported (IQ-TREE bootstrap = 97 % / RAxML bootstrap = 100 % / PP = 1), respectively. No *CaM* sequence is available for the ex-type isolate of *F. brachygibbosum* (NRRL 20954) and therefore a comparison was made with the sequence of isolate NRRL 34033. The *CaM* sequence of isolate LLC1803 is 99.29 % (559/563 nt) identical to *F. brachygibbosum* isolate NRRL 34033, the *rpb1* sequence 99.44 % (881/886 nt), the *rpb2* sequence 98.45 % (888/902 nt), and the *tef1* sequence 97.74 % (605/619 nt).

Fusarium pentaseptatum Crous, Sand.-Den. & M.M. Costa, *sp. nov*. MycoBank MB 846719. Fig. 21.

Etymology: Name refers to its predominantly 5-septate macroconidia.

Typus: **Ethiopia**, Tigray Region, Western (Mirab) Zone, Tahtay Adiyabo District, Kushet locality (Kebele), endophytic from seed of *Striga hermonthica*, 2017, *T. Tessema & L. Lombard* (**holotype** EMCC-F321, preserved as metabolically inactive culture, culture ex-type LLC1022 = EMCC-F321).

Aerial conidiophores not observed. *Sporodochia* pale luteous, abundant on CLA. *Sporodochial conidiophores* densely aggregated, branched, consisting of a stipe bearing whorls or 2–4 monophialides; *sporodochial conidiogenous cells* monophialidic, doliiform to subcylindrical, 8–13 × 4–5 µm, smooth- and thin-walled with periclinal thickening at apex. *Sporodochial conidia* falcate, curved dorsiventrally, widest in second or third cell from apex; apical cell curved, pointed; basal cell foot-shaped, notch poorly developed, (3–)5-septate, hyaline, smooth-walled, guttulate; 4-septate conidia (32–)34–36(–38) × 6–7 µm, 5-septate conidia (33–)37–38(–45) × 6–7 µm. *Chlamydospores* on SNA after 1 wk, solitary or in pairs, terminal or intercalary, subglobose, 12–15 µm diam.

Culture characteristics: Colonies erumpent, spreading, covering dish after 7 d at 25 °C. On PDA surface rosy vinaceous to vinaceous, reverse scarlet to violet; on OA surface and reverse pale luteous.

Additional materials examined: Supplementary Table S1.

Notes: *Fusarium pentaseptatum* FSAMSC 28 (*F. sambucinum* SC) (Fig. 2) is fully supported in all three analyses and a sister clade to *F. subflagellisporum*; the node joining the two clades is only fully supported in the Bayesian analysis. This lineage was introduced by Laraba *et al.* (2021) as "F. sp. nov.-28" for two isolates from China, associated with soil and soybean roots, respectively. The authors did not formally name this clade and therefore a name is introduced in the present study. The phylogenetic tree shows two potential subclades; however, these differences are minor (comparison of NRRL 66939 with LLC1020; *CaM*: no sequences for NRRL 66939 & FRC R-9121 to compare; *rpb1*: 883/886 nt; *rpb2*: 898/902 nt; *tef1*: 609/612 nt). No *CaM* and *rpb1* sequences are available for the ex-type isolate of *F. subflagellisporum* (COAD 2989). The *rpb2* sequence of isolate LLC1020 is 95.23 % (859/902 nt) identical to the ex-type isolate of *F. subflagellisporum* (COAD 2989). The *tef1* sequence of isolate LLC1020 is 97.03 % (653/673 nt) identical to the ex-type isolate of *F. subflagellisporum* (COAD 2989). A comparison was also made against the ex-type of *F. brachygibbosum* (NRRL 20954): *CaM*: no sequences for NRRL 20954 to compare; *rpb1*: 868/886 nt; *rpb2*: 877/900 nt; *tef1*: 593/617 nt.

Fusarium subflagellisporum T.F. Nóbrega & R.W. Barreto, *Persoonia* **47**: 313. 2021.

Materials examined: Supplementary Table S1.

Notes: The isolates cluster with the ex-type of *F. subflagellisporum* in a fully-supported clade (Fig. 2). *Fusarium subflagellisporum* is listed as FSAMSC 27 in Laraba *et al.* (2021).

Fusarium transvaalense Sand.-Den. *et al.*, *MycoKeys* **34**: 82. 2018.

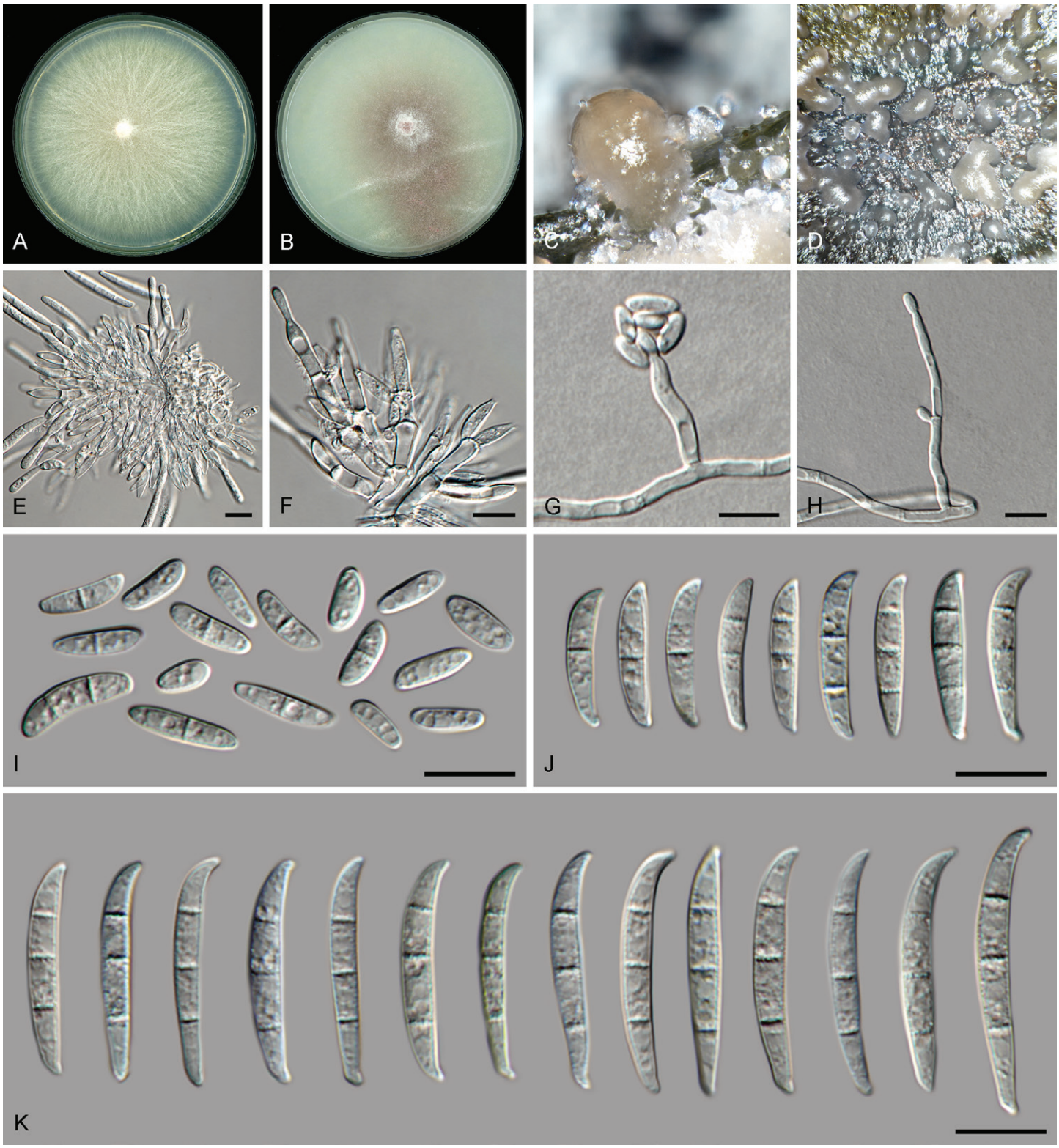

Fig. 19. *Fusarium veterinarium* (LLC 3929). **A.** Colony on PDA. **B.** Colony on OA. **C, D.** Sporodochia on carnation leaves. **E, F.** Sporodochia and sporodochial conidiophores. **G.** False head carried on a phialide on aerial mycelium. **H.** Conidiophore and phialides on aerial mycelium. **I.** Aerial microconidia. **J.** Aerial macroconidia. **K.** Sporodochial macroconidia. Scale bars = 10 µm.

Materials examined: Supplementary Table S1.

Notes: In the phylogenetic tree (Fig. 2), the *F. transvaalense s.l.* clade is fully supported and the two internal subclades were fully and highly supported (IQ-TREE bootstrap = 99 % / RAxML bootstrap = 87 % / PP = 1), respectively. The *rpb1* sequence of isolate LLC1488 is 99.24 % (131/132 nt) identical to the ex-type isolate of *F. transvaalense* (CBS 144211) – only partial overlap is available for comparison. The *rpb2* sequence of isolate LLC1488 is 98.56 % (889/902 nt) identical to the ex-type isolate of *F. transvaalense* (CBS 144211), and the *tef1* sequence 96.75 % (655/677 nt).

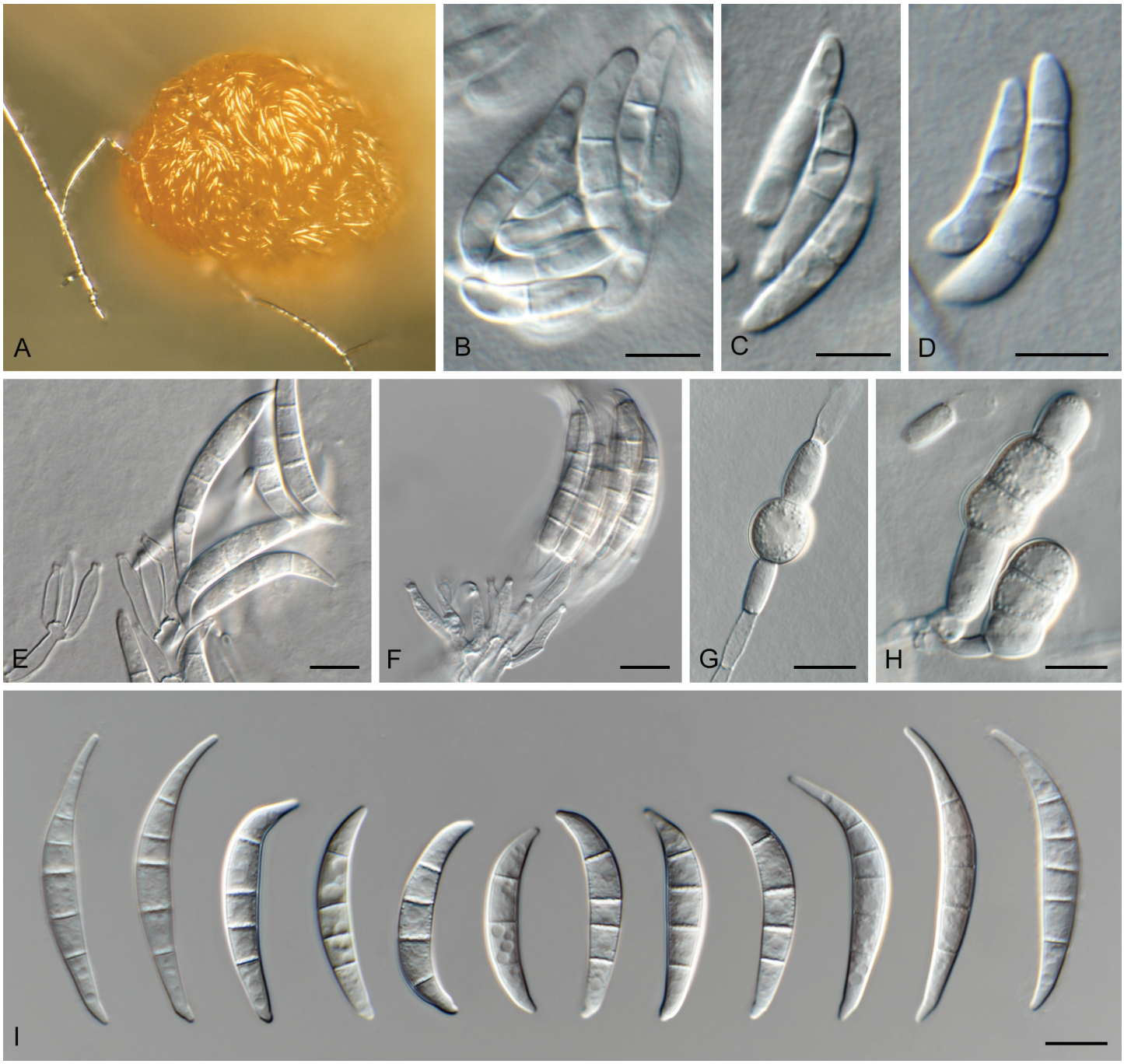

Fig. 20. *Fusarium brachygibbosum* (LLC 1803). **A.** Sporodochium on SNA. **B–D.** Macroconidia submerged in SNA. **E, F.** Sporodochial conidiophores. **G, H.** Chlamydospores. **I.** Sporodochial macroconidia. Scale bars = 10 µm.

Fusarium tricinctum species complex (FTSC)

Fusarium avenaceum (Fr.) Sacc., *Syll. Fung*. **4**: 713. 1886.
Synonyms: see www.fusarium.org

Materials examined: Supplementary Table S1.
Notes: Isolate LLC725 clusters with isolates labelled as *F. avenaceum* and *F. arthrosporioides* (including the ex-neotype of *F. avenaceum*) in the phylogenetic tree (Fig. 2). We choose to place this isolate in *F. avenaceum* for now as there are currently no (ex-)type sequences available for *F. arthrosporioides.*

DISCUSSION

In the present study we investigated which *Fusarium* spp. were associated with soil from *Sorghum* fields in Ethiopia, or dominate the rhizosphere of *Sorghum* when grown in these soils or occurred as endophytes in *Sorghum* roots and seeds, or *Striga* stems and seeds. A total of 42 *Fusarium* species distributed over eight different *Fusarium* Species Complexes were identified, including three species which we believe are new to science and two undescribed species.

Several species complexes were poorly represented, namely FburSC (*F. burgessii*, 1 isolate), FCSC (*F. nelsonii*, 3 isolates and *F. sporodochiale*, 1 isolate), FCOSC (*F. concolor*, 1 isolate), and FTSC (*F. avenaceum*, 1 isolate). *Fusarium burgessii* was initially described from soils associated with native vegetation in

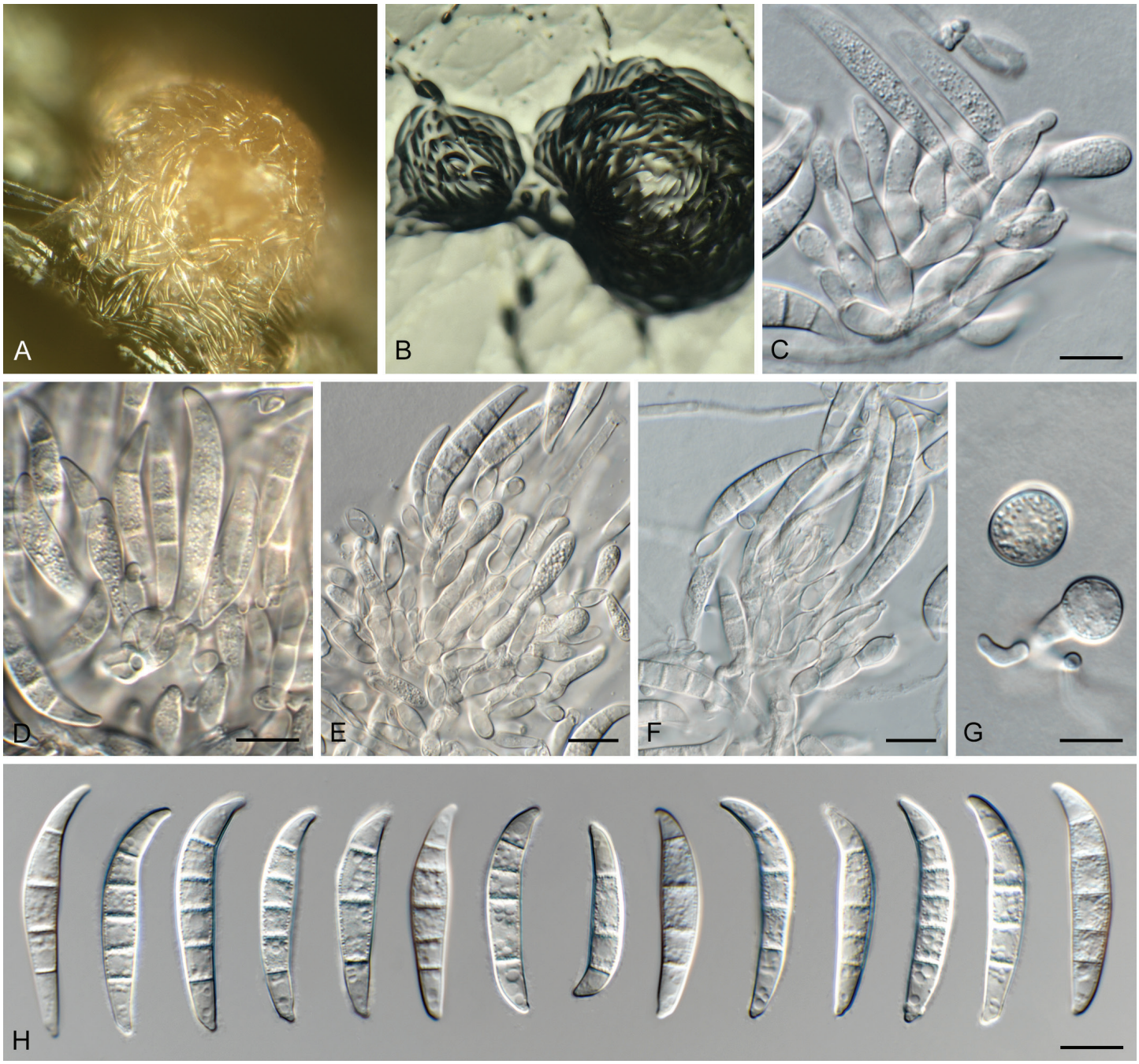

Fig. 21. *Fusarium pentaseptatum* (LLC 1022). **A, B.** Sporodochia on SNA. **C–F.** Sporodochial conidiophores. **G.** Chlamydospores. **H.** Sporodochial macroconidia. Scale bars = 10 µm.

Australia (Laurence *et al.* 2011). *Fusarium nelsonii* was isolated from plant debris in wheat soil, the roots of *Medicago* and from sorghum malt and corn kernels (Marasas *et al*. 1998) and *F. sporodochiale* from soil collected in South Africa (Lombard *et al*. 2019). *Fusarium concolor* (described from *Hordeum vulgare* in Uruguay; Reinking 1934) was recently reported from various soils associated with *Hordeum*, *Triticum* and *Zea* in Africa (South Africa, Zimbabwe), Australia, Europe (Italy, Spain), South America (Uruguay), and North America (Hawaii, Georgia) (Jacobs-Venter *et al.* 2018). Lastly, *F. avenaceum* (neotype from *Hordeum vulgare* in Denmark; Crous *et al.* 2021b) is a common soilborne fungus, and can cause stem and root diseases in various pasture legumes in temperate regions of the world (Leslie & Summerell 2006). Although soilborne, none of these four species were well represented in the present study, and thus probably play a minor role in the *Striga*/*Sorghum* pathosystem.

Four complexes that were well represented however, include the FFSC, FIESC, FOSC and FSAMSC. Fifteen species were delineated in the FFSC. Although *F. proliferatum* has been extensively studied in the past, most isolates were representative of *F. annulatum* (Yilmaz *et al*. 2021). *Fusarium annulatum* is common in tropical and temperate zones, and has been reported from a wide host range (Domsch *et al.* 2007), occurring in various soil samples in the present study. *Fusarium caapi* was recently described from Brazil, where it was isolated from seed of *Brachiaria brizantha* (Costa *et al*. 2021), and this is the first record from Africa, where it was found in *Sorghum* rhizospere soil samples. *Fusarium lactis* was originally identified from clotted milk in Europe, and later shown to be associated with endosepsis of figs in California (Leslie & Summerell 2006),

but was here found associated with *Sorghum* root collors in a Dutch experimental greenhouse. *Fusarium mirum* was recently described from *Sorghum bicolor* in Cameroon and Egypt (Costa *et al*. 2022), and here isolated from *Sorghum* soil and *Striga* seed in Ethiopia. *Fusarium brevicatenulatum* was originally described from symptomatic plants of *Striga asiatica* collected in Madagascar (Nirenberg *et al.* 1998), and shown here to be synonymous with *F. pseudoanthophilum* (*Zea mays*, Zimbabwe), a synonymy already suspected by Leslie & Summerell (2006), and confirmed via mating studies by Amata *et al.* (2010). The Ethiopian isolates studied here were all recovered from *Striga* seed, again underlining the strong association of *F. brevicatenulatum* with *Striga*. *Fusarium sudanense* was described from *Striga hermonthica* in Sudan (Moussa *et al*. 2017), and later also reported to cause seedling blight and seed rot of wheat in Argentina (Larran *et al.* 2020). The isolates recovered in the present study originated from either *Striga* seed, or *Sorghum* field or rhizosphere soil in Ethiopia. *Fusarium fredkrugeri* was described from soil samples and the rhizosphere of *Melhania acuminata* collected in South Africa, and is also known from *Striga hermonthica* in Madagascar (Sandoval-Denis *et al.* 2018), and isolated from *Striga* seed and *Sorghum* field and rhizosphere soil in Ethiopia in the present study. *Fusarium secorum*, a sugar beet pathogen from the USA (Secor *et al*. 2014), is reported here as a single isolate from *Sorghum* field soil in Ethiopia. *Fusarium udum* causes a wilt disease of *Cajanus cajan* and *Crotalaria* spp. in tropical regions (Pfenning *et al*. 2019), and is reported here from *Sorghum* field soil in Ethiopia. *Fusarium thapsinum* is widely distributed, causing a stalk rot and grain mould of *Sorghum* (Leslie & Summerell 2006), and was also isolated from *Striga* seed and *Sorghum* rhizosphere soil in Ethiopia in this study. *Fusarium verticillioides* is globally widely distributed, causing a stalk and cob rot of maize (Leslie & Summerell 2006), and was isolated from *Sorghum* seed and rhizosphere soil in Ethiopia in the present study. *Fusarium andiyazi* is pathogenic to *Sorghum*, and may be the most dominant *Fusarium* species on this host (Marasas *et al.* 2001). It has also been reported from *Zea mays* in Portugal (Simões *et al.* 2022), and *Saccharum officinarum* in China (Bao *et al*. 2020). It was isolated from *Striga* seed and stems, and *Sorghum* seed in Ethiopia in the present study. *Fusarium ficicrescens,* isolated from figs in Iran (Al-Hatmi *et al.* 2016), is reported here from *Striga asiatica* seed collected in Ethiopia. *Fusarium nygamai* is widely distributed and has been associated with root rot of *Asparagus*, *Gossypium*, *Oryza, Pennisetum*, *Sorghum, Vicia faba* and *Zea*, and may cause systemic infections in humans (Leslie & Summerell 2006). It was isolated from *Sorghum* field and rhizosphere soil in Ethiopia in the present study. The last species in this SC remains unnamed for now (*Fusarium* sp. isolate LLC1198) pending the collection of more isolates.

Ten species were associated with the FIESC, including *F. extenuatum* and *F. tangerinum*, which were described here as new species isolated from Ethiopian *Sorghum* field soil and *Sorghum* seed and rhizosphere, respectively. *Fusarium compactum* is commonly isolated from grasslands and dry dessert soils in hot climates (Australia, Middle East, Africa; Leslie & Summerell 2006), and is generally regarded as a saprobe. In the present study it was isolated from *Striga hermonthica* seed and *Sorghum* field soil in Ethiopia. *Fusarium lacertarum* is known as a pathogen of *Vigna unguiculata* and *Nopalea cochenillifera* in Brazil (do Amaral *et al.* 2022), and *Sorghum bicolor* in the USA (Beacorn & Thiessen 2021). It the present study it was isolated as endophyte from *Sorghum* seed and from *Sorghum* rhizosphere soil in Ethiopia. *Fusarium nanum* was described from *Musa nana* in China (Wang *et al*. 2019), and has since been found to cause decay of *Cucumis melo* in China (Zhang *et al.* 2022), and *Glycine max* in the USA (Okello *et al.* 2020). It was isolated as an endophyte from Ethiopian *Sorghum* seed in the present study. *Fusarium caatingaense*, which was described from insects in Brazil (Santos *et al.* 2019), was isolated as an endophyte from Ethiopian *Striga hermonthica* seed in the present study. *Fusarium serpentinum* was described from an unknown substrate by Xia *et al.* (2019), and isolated in the present study from *Sorghum* rhizosphere soil in Ethiopia. *Fusarium clavus* was described from environmental, plant and human samples originating from Africa, Asia, Europe and North America (Xia *et al*. 2019). It proved to be a dominant taxon in the present study, being isolated as endophyte from *Striga hermonthica* seed as well as *Sorghum* field and rhizosphere soils in Ethiopia. *Fusarium duofalcatisporum* appears to be restricted to North- and South-eastern Africa (O'Donnell *et al.* 2009), and is here shown to be a dominant taxon in the *Striga*/*Sorghum* pathosystem, associated as endophyte with *Striga hermonthica* seed, as well as *Sorghum* field and rhizosphere soil in Ethiopia. *Fusarium incarnatum* has a complicated taxonomic history with numerous synonyms (Xia *et al*. 2019, Crous *et al*. 2021b) and was here isolated from *Striga* and *Sorghum* seeds as well as *Sorghum* rhizosphere soil from Ethiopia.

Eight species are associated with the FOSC. *Fusarium odoratissimum* is the well-known causal agent of Panama disease of banana (Maryani *et al*. 2019a). Surprisingly, an isolate from this pathogen was recently collected during a Citizen Science project sampling garden soils in the Netherlands (Crous *et al*. 2021a), and was again isolated from the roots of *Sorghum* plants growing in Dutch greenhouse soils during the present study. *Fusarium fabacearum* was described from *Glycine max* and Zea mays collected in South Africa (Lombard *et al*. 2019), and was isolated from seed of *Striga asiatica* and *Sorghum* field and rhizosphere soils in Ethiopia in the present study. *Fusarium veterinarium* was reported from diverse, mainly veterinary samples collected in Europe and the USA (Lombard *et al*. 2019), and shown to be common in Ethiopian as well as Dutch *Sorghum* rhizosphere soil in the present study. *Fusarium curvatum* is known from *Beaucarnia* sp., *Hedera helix* and *Matthiola incana* collected in Europe, and reported here as a single isolate from *Sorghum* field soil in Ethiopia. *Fusarium libertatis* was described from the rock surfaces in the stone quarry on Robben Island (Van Riebeeck's Quarry), where Nelson Mandela and other political prisoners were forced to undergo manual hard labour. This species is here also reported as a single isolate from *Sorghum* field soil in Ethiopia. *Fusarium glycines* is known from *Glycine max* collected in South Africa and *Linum usitatissium* from an unknown location (Lombard *et al.* 2019), while *F. gossypinum* is known from wilted *Gossypium hirsutum* collected in the Ivory coast; both species were isolated here from *Sorghum* field and rhizosphere soil in Ethiopia. *Fusarium* sp. 1 is an unnamed species in the FOSC from garden soil in the Netherlands (Crous *et al*. 2021a) and was also isolated from *Sorghum* roots in a Dutch greenhouse.

Four species are associated with FSAMSC in this study. *Fusarium brachygibbosum* was originally described from diseased *Sorghum vulgare* plants collected in India (Crous *et al.* 2021b), and is now regarded as a a potential European Union quarantine pest (EFSA PLH Panel 2021). In the present

study it was isolated from *Sorghum* field soil in Ethiopia. *Fusarium pentaseptatum* (=FSAMSC 28; Laraba *et al.* 2021) is described here as endophyte from *Striga hermonthica* seed and *Sorghum* field and rhizosphere soils in Ethiopia, and is known from soybeans and soil samples in China (Laraba *et al.* 2021). *Fusarium subflagellisporum* (=FSAMSC 27; Laraba *et al.* 2021) was described based on hypertrophied floral and vegetative branches of *Mangifera indica* trees in Brazil, but has been reported from *Arachis hypogaea* and *Zea mays* soil in the USA, *Sorghum* debris in Puerto Rico, from Nigeria, and *Pennisetum* soils in Zimbabwe (Crous *et al.* 2021b). In the present study it is reported from Ethiopian *Striga hermonthica* seed and *Sorghum* field soil. Lastly, *Fusarium transvaalense* is known from the rhizosphere of *Sida cordifolia*, *Kyphocarpa angustifolia* and *Melhania acuminata* in South Africa (Sandoval-Denis *et al*. 2018), and is reported here from Ethiopian *Sorghum* field and rhizosphere soil.

Zimmermann *et al*. (2015) developed a specific AFLP-based marker to identify isolates of *F. oxysporum f.sp. strigae* (Fos) among other *Fusarium* isolates isolated from *Striga hermonthica* collected in Africa (Burkina Faso, Ghana, Kenya, Mali, Nigeria and Niger). Barring one isolate of *F. oxysporum f.sp. melonis* from Israel, the test proved highly effective in detecting this DNA fragment in isolates of Fos, suggesting it an effective marker to use in the detection of Fos in African soils. In screening for this marker DNA fragment among the isolates obtained in the present study, however, it was detected in several species in diverse species complexes, namely (FCSC) *F. nelsonii*; (FFSC) *F. andiyazi*, *F. annulatum*, *F. fredkrugeri*, *F. nygamai*, *F. sudanense*, *F. verticillioides*; (FIESC) *F. clavus*, *F. compactum*, *F. duofalcatisporum*, *F. lacertarum*; (FOSC) *F. fabacearum*, *F. glycines*, *F. veterinarium* and (FSAMSC) *F. brachygibbosum*, *F. subflagellisporum* and *F. transvaalense*. Interestingly, many isolates from the FSAMSC contain a positive amplicon with a sequence which is not completely identical to the original reference sequence (19 substitutions over the length of 165 nucleotides). Although it is to be expected that the AFLP-based marker DNA fragment could be transferred among isolates in the FOSC via the parasexual cycle (Ma *et al.* 2010), it is rather surprising to find it in other *Fusarium* species complexes, suggesting that the parasexual cycle (or horizontal chromosome transfer) could be more prominent in *Fusarium* than expected. Further studies are now underway to determine if the presence of this DNA fragment also correlates with effective biocontrol of *Striga*, as it does in the case of Fos. Further research is therefore required to establish the potential role that these various *Fusarium* spp. could play in inhabiting *Striga*.

ACKNOWLEDGEMENTS

The Bill and Melinda Gates Foundation supported this research work through grant number OPP1082853: PROMISE 'Promoting Root Microbes for Integrated *Striga* Eradication' project via Ethiopian Institute of Agricultural Research and Netherlands Institute of Ecology. We thank Marjan Vermaas for assistance with the photographic plates.

Conflict of interest: The authors declare that there is no conflict of interest.

REFERENCES

Abbasher AA, Kroschel J, Sauerborn J (1995). Micro-organisms of *Striga hermonthica* in northern Ghana with potential as biocontrol agents. *Biocontrol Science and Technology* **5**: 157–161.

Abbasher AA, Sauerborn J (1992). *Fusarium nygamai* a potential bioherbicide for *Striga hermonthica* control in sorghum. *Biological Control* **2**: 291–296.

Abbasher AA, Sauerborn J, Kroschel J, *et al.* (1996). Evaluation of *Fusarium semitectum var. majus* for biological control of *Striga hermonthica*. In: *Ninth International Symposium on Biological Control of Weeds* (Moran VC, Hoffmann JH, eds). University of Cape Town, South Africa: 115–120.

Al-Hatmi AMS, Mirabolfathy M, Hagen F, *et al*. (2016). DNA barcoding, MALDI-TOF, and AFLP data support *Fusarium ficicrescens* as a distinct species within the *Fusarium fujikuroi* species complex. *Fungal Biology* **120**: 265–278.

Amata RL, Burgess LW, Summerell BA, *et al.* (2010). An emended description of *Fusarium brevicatenulatum* and *F. pseudoanthophilum* based on isolates recovered from millet in Kenya. *Fungal Diversity* **43**: 11–25.

Anteyi WO, Klaiber I, Rasche F (2022). Diacetoxyscirpenol, a *Fusarium* exometabolite, prevents efficiently the incidence of the parasitic weed *Striga hermonthica*. *BMC Plant Biology* **22**: 84.

Bao Y, Huang Z, Li T, *et al*. (2020). First report of *Fusarium andiyazi* causing sugarcane Pokkah Boeng Disease in China. *Plant Disease* **104**: 286–286.

Beacorn JA, Thiessen LD (2021). First report of *Fusarium lacertarum* causing Fusarium Head Blight on *Sorghum* in North Carolina. *Plant Disease* **105**: 699.

Ciotola M, DiTommaso A, Watson AK (2000). Chlamydospore production, inoculation methods and pathogenicity of *Fusarium oxysporum* M12-4A, a biocontrol for *Striga hermonthica*. *Biocontrol Science and Technology* **10**: 129–145.

Ciotola M, Watson AK, Hallett SG (1995). Discovery of an isolate of *Fusarium oxysporum* with potential to control *Striga hermonthica* in Africa. *Weed Research* **35**: 303–309.

Costa MM, Melo MP, Sandin FC, *et al.* (2021). *Fusarium* species from tropical grasses and description of two new taxa. *Mycological Progress* **20**: 61–72.

Costa MM, Saleh AA, Melo MP, *et al*. (2022). *Fusarium mirum sp. nov*., intertwining *Fusarium madaense* and *Fusarium andiyazi*, pathogens of tropical grasses. *Fungal Biology* **126**: 250–266.

Crous PW, Gams W, Stalpers JA, *et al.* (2004). MycoBank: an online initiative to launch mycology into the 21st century. *Studies in Mycology* **50**: 19–22.

Crous PW, Hernández-Restrepo M, van Iperen AL, *et al.* (2021a). Citizen science project reveals novel fusarioid fungi (*Nectriaceae, Sordariomycetes*) from urban soils. *Fungal Systematics and Evolution* **8**: 101–127.

Crous PW, Lombard L, Sandoval-Denis M, *et al.* (2021b). *Fusarium*: more than a node or a foot-shaped basal cell. *Studies in Mycology* **98**: 100116.

Crous PW, Verkleij GJM, Groenewald JZ, *et al.* (2019). Fungal Biodiversity. [Westerdijk Laboratory Manual Series No. 1]. Westerdijk Fungal Biodiversity Institute publishing, Utrecht, Netherlands.

Daffalla HM, Hassan MM, Osman MG, *et al.* (2014). Effect of seed priming on early development of *Sorghum* (*Sorghum bicolor* L. Moench) and *Striga hermonthica* (Del.) Benth. *International Scholarly Research Notices* **2014**: 134931.

do Amaral ACT, Koroiva R, da Costa AF, *et al.* (2022). First report of *Fusarium lacertarum* as the causal agent of wilt in *Vigna*

unguiculata. *Journal of Plant Pathology* **104**: 1173.

Domsch K, Gams W, Anderson T-H (2007). *Compendium of Soil Fungi* 2 edn. IHW-Verlag, Eching.

EFSA PLH Panel (EFSA Panel on Plant Health), Bragard C, Di Serio F, Gonthier P, *et al.* (2021). Scientific Opinion on the pest categorisation of *Fusarium brachygibbosum*. *EFSA Journal* **19**: 6887.

Ejeta G (2007). Breeding for *Striga* resistance in sorghum: exploitation of an intricate host–parasite biology. *Crop Science* **47** (Suppl. 3): S216–S227.

Fisher NL, Burgess LW, Toussoun TA, *et al*. (1982). Carnation leaves as a substrate and for preserving cultures of *Fusarium* species. *Phytopathology* **72**: 151–153.

Giraldo A, Hernández-Restrepo M, Crous PW (2019). New plectosphaerellaceous species from Dutch garden soil. *Mycological Progress* **18**: 1135–1154.

Gressel J, Hanafi A, Head G, *et al*. (2004). Major heretofore intractable biotic conisolatets to African food security that may be amenable to novel biotechnological solutions. *Crop Protection* **23**: 661–689.

Groenewald M, Lombard L, de Vries M, *et al.* (2018). Diversity of yeast species from Dutch garden soil and the description of six novel Ascomycetes. *Federation of European Microbiological Societies Yeast Research* **18**: foy076.

Gurney AL, Press MC, Scholes JD (2002). Can wild relatives of sorghum provide new sources of resistance or tolerance against *Striga* species? *Weed Research* **42**: 317–324.

Hess DE, Kroschel J, Traoré D, *et al.* (2002). *Striga*: biological control strategies for a new millennium. In: *Sorghum and Millet Diseases 2000* (Leslie JF, ed.), Iowa State Press, Ames, Iowa, USA: 165–170.

Jacobs-Venter A, Laraba I, Geiser DM, *et al*. (2018). Molecular systematics of two sister clades, the *Fusarium concolor* and *F. babinda* species complexes, and the discovery of a novel microcycle macroconidium–producing species from South Africa. *Mycologia* **110**: 1189–1204.

Kroschel J, Hundt A, Abbasher A, *et al.* (1996). Pathogenicity of fungi collected in northern Ghana to *Striga hermonthica*. *Weed Research* **36**: 515–520.

Kroschel J, Jost A, Sauerborn J (1999). Insects for Striga control – possibilities and conisolatets. In: *Advances in Parasitic Weed Control at On-farm Level*. *Vol. I. Joint Action to Control Striga in Africa* (Kroschel J, Mercer-Quarshie H, Sauerborn J, eds.), Margraf Verlag, Weikersheim, Germany: 117–132.

Laraba I, McCormick SP, Vaughan MM, *et al*. (2021). Phylogenetic diversity, trichothecene potential, and pathogenicity within *Fusarium sambucinum* species complex. *PLoS ONE* **16**: e0245037.

Larran S, Siurana MPS, Caselles JR, *et al*. (2020). *Fusarium sudanense*, endophytic fungus causing typical symptoms of seedling blight and seed rot on wheat. *Journal of King Saud University – Science* **32**: 468–474.

Laurence MH, Summerell BA, Burgess LW, *et al*. (2011). *Fusarium burgessii sp. nov*. representing a novel lineage in the genus *Fusarium*. *Fungal Diversity* **49**: 101–112.

Leslie JF, Summerell BA (2006). *The* Fusarium *laboratory manual*. Blackwell Publishing Professional, USA.

Lombard L, Sandoval-Denis M, Lamprecht SC, *et al*. (2019). Epitypification of *Fusarium oxysporum* – clearing the taxonomic chaos. *Persoonia* **43**: 1–47.

Ma L, van der Does HC, Borkovich KA, *et al*. (2010). Comparative genomics reveals mobile pathogenicity chromosomes in *Fusarium*. *Nature* **464**: 367–373.

Marasas WFO, Rheeder JP, Lamprecht SC, *et al.* (2001). *Fusarium andiyazi sp. nov*., a new species from sorghum. *Mycologia* **93**: 1203–1210.

Marasas WFO, Rheeder JP, Logrieco A, *et al*. (1998). *Fusarium nelsonii* and *F. musarum*: two new species in Section *Arthrosporiella* related to *F. camptoceras*. *Mycologia* **90**: 505–513.

Marley PS, Aba DA, Shebayan JAY, *et al.* (2004). Integrated management of *Striga hermonthica* in sorghum using a mycoherbicide and host plant resistance in the Nigerian Sudano-Sahelian savanna. *Weed Research* **44**: 157–162.

Marley PS, Ahmed SM, Shebayan JAY, *et al.* (1999). Isolation of *Fusarium oxysporum* with potential for biocontrol of the witchweed (*Striga hermonthica*) in the Nigerian Savanna. *Biocontrol Science and Technology* **9**: 159–163.

Maryani N, Lombard L, Poerba YS, *et al*. (2019a). Phylogeny and genetic diversity of the banana Fusarium wilt pathogen *Fusarium oxysporum f. sp. cubense* in the Indonesian centre of origin. *Studies in Mycology* **92**: 155–194.

Maryani N, Sandoval-Denis M, Lombard L, *et al*. (2019b). New endemic *Fusarium* species hitch-hiking with pathogenic *Fusarium* isolates causing Panama disease in small-holder banana plots in Indonesia. *Persoonia* **43**: 48–69.

Masteling R, Lombard L, de Boer W, *et al.* (2019). Harnessing the microbiome to control plant parasitic weeds. *Current Opinion in Microbiology* **49**: 26-33.

Minh Q, Schmidt HA, Chernomor O, *et al*. (2020). IQ-TREE2: new models and efficient methods for phylogenetic inference in the genomic era. *Molecular Biology and Evolution* **37**: 1530–1534.

Moussa TAA, Al-Zharani HS, Kadasa NMS, *et al*. (2017). Two new species of the *Fusarium fujikuroi* species complex isolated from the natural environment. *Antonie van Leeuwenhoek* **110**: 819–832.

Nguyen LT, Schmidt HA, von Haeseler A, *et al*. (2015). IQ-TREE: a fast and effective stochastic algorithm for estimating maximum-likelihood phylogenies. *Molecular Biology and Evolution* **32**: 268–274.

Nirenberg H, O'Donnell K, Kroschel J, *et al*. (1998). Two new species of *Fusarium*: *Fusarium brevicatenulatum* from the noxious weed *Striga asiatica* in Madagascar and *Fusarium pseudoanthophilum* from *Zea mays* in Zimbabwe. *Mycologia* **90**: 459–463.

Nirenberg HI (1976). Untersuchungen über die morphologische und biologische Differenzierung in der *Fusarium*-Sektion *Liseola*. *Mitteilungen aus der Biologischen Bundesanstalt für Land- und Forstwirtschaft Berlin-Dahlem* **169**: 1–117.

O'Donnell K, Sutton DA, Rinaldi MG, *et al*. (2009). Novel multilocus sequence typing scheme reveals high genetic diversity of human pathogenic members of the *Fusarium incarnatum-equiseti* and *F. chlamydosporum* species complexes within the United States. *Journal of Clinical Microbiology* **47**: 3851–3861.

Okello PN, Petrovic K, Singh AK, *et al.* (2020). Characterization of species of *Fusarium* causing root rot of Soybean (*Glycine max* L.) in South Dakota, USA, *Canadian Journal of Plant Pathology* **42**: 560–571.

Parker C (2012). Parasitic Weeds: A world Challenge. *Weed Science* **60**: 269–276.

Pfenning LH, De Melo MP, Costa MM, *et al*. (2019). *Fusarium udum* revisited: a common, but poorly understood member of the *Fusarium fujikuroi* species complex. *Mycological Progress* **18**: 107–117.

Rayner RW (1970). *A mycological colour chart*. CMI and British Mycological Society, Kew, Surrey, UK.

Reinking OA (1934). Interesting new *Fusaria*. *Zentralblatt für Bakteriologie und Parasitenkunde, Abteilung 2.* **89**: 509–514.

Ronquist F, Huelsenbeck JP (2003). MrBayes 3: Bayesian phylogenetic inference under mixed models. *Bioinformatics* **19**: 1572–1574.

Sandoval-Denis M, Swart WJ, Crous PW (2018). New *Fusarium* species from the Kruger National Park, South Africa. *MycoKeys* **34**: 63–92.

Santos ACDS, Trindade JVC, Lima CS, *et al*. (2019). Morphology,

phylogeny, and sexual stage of *Fusarium caatingaense* and *Fusarium pernambucanum*, new species of the *Fusarium incarnatum-equiseti* species complex associated with insects in Brazil. *Mycologia* **111**: 244–259.

Sauerborn J, Abbasher AA, Kroschel J, *et al.* (1996). Biological control of *Striga hermonthica* with *Fusarium nygamai* in maize. In: *Ninth International Symposium on Biological Control of Weeds* (Moran VC, Hoffmann JH, eds), University of Cape Town, South Africa: 461–466.

Sauerborn J, Müller-Stöver D, Hershenhorn J (2007). The role of biological control in managing parasitic weeds. *Crop Protection* **26**: 246–254.

Secor GA, Rivera-Varas V, Christ DS, *et al*. (2014). Characterization of *Fusarium secorum*, a new species causing Fusarium yellowing decline of sugar beet in north central USA. *Fungal Biology* **118**: 764–75.

Simões D, Diogo E, de Andrade E (2022). First report of *Fusarium andiyazi* presence in Portuguese maize kernels. *Agriculture* **12**: 336.

Stamatakis A (2014). RAxML version 8: a tool for phylogenetic analysis and post-analysis of large phylogenies. *Bioinformatics* **30**: 1312–1313.

Vurro M, Boari A, Thiombiano B, *et al*. (2019). Strigolactones and parasitic plants. In: *Strigolactones - Biology and Applications* (Koltai H, Prandi C, eds). Springer International Publishing: 89–120.

Wang MM, Chen Q, Diao YZ, *et al*. (2019). *Fusarium incarnatum-equiseti* complex from China. *Persoonia* **43**: 70–89.

Xia JW, Sandoval-Denis M, Crous PW, *et al*. (2019). Numbers to names – restyling the *Fusarium incarnatum-equiseti* species complex. *Persoonia* **43**: 186–221.

Yilmaz N, Sandoval-Denis M, Lombard L, *et al.* (2021). Redefining species limits in the *Fusarium fujikuroi* species complex. *Persoonia* **46**: 129–162.

Zhang XP, Dang QQ, Cao XD, *et al*. (2022). First report of muskmelon fruit rot caused by *Fusarium nanum* in China. *Plant Disease* **106**: 1763.

Zhang Z, Schwartz S, Wagner L, *et al*. (2000). A greedy algorithm for aligning DNA sequences. *Journal of Computational Biology* **7**: 203–214.

Zimmermann J, de Klerk M, Musyoki MK, *et al.* (2015). An explicit AFLP-based marker for monitoring *Fusarium oxysporum f.sp. strigae* in tropical soils. *Biological Control* **89**: 42–52.

Supplementary Material: http://fuse-journal.org/

Table S1. Collection details, striga gene haplotype and GenBank accession numbers of novel strains used in the phylogenetic trees.

Table S2. Collection details and GenBank accession numbers of strains used in the phylogenetic trees.

Table S3. Summary of phylogenetic information for the different analyses in this study.